Published for SISSA by Springer

Received: November 22, 2019
Accepted: February 25, 2020
Published: March 18, 2020

Search for lepton flavour violating decays of a neutral heavy Higgs boson to $\mu\tau$ and $e\tau$ in proton-proton collisions at $\sqrt{s} = 13$ TeV

The CMS collaboration

E-mail: cms-publication-committee-chair@cern.ch

Abstract: A search for lepton flavour violating decays of a neutral non-standard-model Higgs boson in the $\mu\tau$ and $e\tau$ decay modes is presented. The search is based on proton-proton collisions at a center of mass energy $\sqrt{s} = 13$ TeV collected with the CMS detector in 2016, corresponding to an integrated luminosity of 35.9 fb^{-1}. The τ leptons are reconstructed in the leptonic and hadronic decay modes. No signal is observed in the mass range 200–900 GeV. At 95% confidence level, the observed (expected) upper limits on the production cross section multiplied by the branching fraction vary from 51.9 (57.4) fb to 1.6 (2.1) fb for the $\mu\tau$ and from 94.1 (91.6) fb to 2.3 (2.3) fb for the $e\tau$ decay modes.

Keywords: Hadron-Hadron scattering (experiments), Higgs physics

ArXiv ePrint: 1911.10267

https://doi.org/10.1007/JHEP03(2020)103

JHEP03(2020)103

Contents

1 Introduction

The discovery of the 125 GeV Higgs boson, H(125), at the CERN LHC in 2012 [1–3] was a major breakthrough in particle physics. A combined study of data from collisions at $\sqrt{s} =$ 7 and 8 TeV collected by the ATLAS and CMS Collaborations shows the particle to have properties consistent with the standard model (SM) Higgs boson [4–9] including the spin, couplings, and charge-parity assignment [10, 11]. Lepton flavour violating (LFV) decays of the H(125) are forbidden in the SM. However, the presence of new physics in the Higgs sector is not excluded [12] and there exist many possible extensions of the SM that allow LFV decays of the H(125). These include the two Higgs doublet model [13], supersymmetric models [14–20], composite Higgs models [21, 22], models with flavour symmetries [23], Randall-Sundrum models [24–26], and others [27–35]. A common feature of many of these models is the presence of additional neutral Higgs bosons (H and A) that would also have LFV decays [36, 37].

The most recent search for LFV decays of the H(125) was performed by the CMS Collaboration in the $\mu\tau$ and $e\tau$ channels, using proton-proton (pp) collision data recorded

JHEP03(2020)103

at a centre-of-mass energy of $\sqrt{s} = 13\,\text{TeV}$, and corresponding to an integrated luminosity of $35.9\,\text{fb}^{-1}$ [38]. The observed (expected) upper limits set on the branching fractions were $\mathcal{B}(\text{H}(125) \to \mu\tau) < 0.25\,(0.25)\%$ and $\mathcal{B}(\text{H}(125) \to \text{e}\tau) < 0.61\,(0.37)\%$ at 95% confidence level (CL). These constraints were a significant improvement over the previously set limits by the CMS and ATLAS Collaborations using the 8 TeV pp collision data set, corresponding to an integrated luminosity of $20\,\text{fb}^{-1}$ [39–42]. Results from the previous CMS $\text{H}(125) \to \mu\tau$ search, performed using 8 TeV pp collision data, were used to set limits on high mass LFV H decays in a phenomenological study [12]. Limits on the product of the production cross section with branching fraction for the $\text{H} \to \mu\tau$ channel were obtained for H mass, m_{H}, less than 300 GeV.

This paper describes the first direct search for LFV $\text{H} \to \mu\tau$ and $\text{H} \to \text{e}\tau$ decays for an H mass in the range $200 < m_{\text{H}} < 900\,\text{GeV}$. The search is performed in four decay channels, $\text{H} \to \mu\tau_{\text{h}}$, $\text{H} \to \mu\tau_{\text{e}}$, $\text{H} \to \text{e}\tau_{\text{h}}$, and $\text{H} \to \text{e}\tau_{\mu}$ where τ_{h}, τ_{e}, and τ_{μ} correspond to the hadronic, electronic and muonic decay channels of τ leptons, respectively. The final-state signatures are very similar to those of the $\text{H} \to \tau\tau$ decays, studied by CMS [43–46] and ATLAS [47]. However, there are some significant kinematic differences. The primary difference is that the muon (electron) in the LFV $\text{H} \to \mu(\text{e})\tau$ decay is produced promptly, and tends to have a higher momentum than in the $\text{H} \to \tau_{\mu(\text{e})}\tau$ decay. Only the gluon fusion production process is considered in this search and the signal is modelled assuming a narrow width of the Higgs boson. The strategy is similar to the previous LFV H(125) searches performed by the CMS Collaboration, but optimised for higher mass Higgs boson decays.

This paper is organized as follows. After a brief overview of the CMS detector in section 2 and the description of the collision data and simulated samples used in the analysis in section 3, the event reconstruction is described in section 4. The event selection is outlined in section 5 and the background processes are described in section 6. This is followed by a description of the systematic uncertainties in section 7. Finally, the results are presented in section 8, and the paper is summarized in section 9.

2 The CMS detector

A detailed description of the CMS detector, together with a definition of the coordinate system used and the relevant kinematic variables, can be found in ref. [48]. The central feature of the CMS apparatus is a superconducting solenoid of 6 m internal diameter, providing a magnetic field of 3.8 T. Within the solenoid volume are a silicon pixel and strip tracker, a lead tungstate crystal electromagnetic calorimeter (ECAL), and a brass and scintillator hadron calorimeter (HCAL), each composed of a barrel and two endcap sections. Forward calorimeters extend the pseudorapidity (η) coverage provided by the barrel and endcap detectors. Muons are detected in gas-ionization chambers embedded in the steel flux-return yoke outside the solenoid. Events of interest are selected using a two-tiered trigger system [49]. The first level, composed of custom hardware processors, uses information from the calorimeters and muon detectors to select events at a rate of around 100 kHz within a time interval of less than 4 μs. The second level, known as the high-level trigger, consists of

JHEP03(2020)103

a farm of processors running a version of the full event reconstruction software optimised for fast processing, and reduces the event rate to around 1 kHz before data storage.

3 Collision data and event simulation

The data used in this analysis have been collected in pp collisions at the LHC, at a centre-of-mass energy of 13 TeV, with the CMS detector in 2016, and correspond to an integrated luminosity of 35.9 fb^{-1} [50]. A trigger requiring at least one muon is used to collect the data sample in the $\text{H} \to \mu\tau_\text{h}$ and $\text{H} \to \mu\tau_\text{e}$ channels. Triggers requiring at least one electron, or a combination of an electron and a muon are used for the $\text{H} \to \text{e}\tau_\text{h}$ and $\text{H} \to \text{e}\tau_\mu$ channels respectively. Simulated samples of signal and background events are produced with different event generators. The $\text{H} \to \mu\tau$ and $\text{H} \to \text{e}\tau$ decay samples are generated with POWHEG 2.0 [51–56] at next-to-leading-order (NLO) in perturbative quantum chromodynamics. Only the gluon fusion (ggH) [57] production mode has been considered in this analysis. These scalar boson samples are generated assuming the narrow width approximation for a range of masses from 200 to 900 GeV. The Z+jets and W+jets processes are simulated using the MADGRAPH5_aMC@NLO 2.2.2 [58] generator at leading order with the MLM jet matching and merging [59]. The MADGRAPH5_aMC@NLO generator is also used for diboson production which is simulated at NLO with the FxFx jet matching and merging scheme [60]. The POWHEG 2.0 and 1.0 at NLO are used for top quark-antiquark ($\text{t}\bar{\text{t}}$) and single top quark production, respectively. The POWHEG and MADGRAPH5_aMC@NLO generators are interfaced with PYTHIA 8.212 [61] for parton showering and fragmentation. The PYTHIA parameters for the underlying event description are set to the CUETP8M1 tune [62]. The set of parton distribution functions (PDFs) used is NNPDF30nloas0118 [63]. The CMS detector response is modelled using GEANT4 [64].

Because of the high instantaneous luminosities attained during data taking, events have multiple pp interactions per bunch crossing (pileup). This effect is taken into account in simulated samples, by generating concurrent minimum bias events, and overlapping them with simulated hard events. All simulated samples are weighted to match the pileup distribution observed in data, which has an average of approximately 23 interactions per bunch crossing.

4 Event reconstruction

The event reconstruction is performed using a particle-flow (PF) algorithm, which aims to reconstruct and identify each individual particle in an event (PF candidate), with an optimised combination of information from the various elements of the CMS detector [65]. In this process, the identification of the particle type for each PF candidate (photon, electron, muon, charged or neutral hadron) plays an important role in the determination of the particle direction and energy. The primary pp vertex of the event is identified as the reconstructed vertex with the largest value of summed physics-object p_T^2, where p_T is the transverse momentum. The physics objects are the jets, clustered using the jet finding

JHEP03(2020)103

algorithm [66, 67] with the tracks assigned to the vertex as inputs, and the associated missing transverse momentum, taken as the negative vector sum of the p_{T} of those jets.

A muon is identified as a track in the silicon detectors, consistent with the primary pp vertex and with either a track or several hits in the muon system, associated with an energy deposit in the calorimeters compatible with the expectations for a muon [65, 68]. Identification is based on the number of spatial points measured in the tracker and in the muon system, the track quality, and its consistency with the event vertex location. The identification working point chosen for this analysis reconstructs muons with an efficiency above 98% and a hadron misidentification rate of 0.1% for pions and 0.3% for kaons. The energy is obtained from the corresponding track momentum. An important aspect of muon reconstruction is the lepton isolation that is described later in this section.

An electron is identified as a charged-particle track from the primary pp vertex in combination with one or more ECAL energy clusters. These clusters are matched with the track extrapolation to the ECAL and with possible bremsstrahlung photons emitted when interacting with the material of the tracker [69]. Electron candidates are accepted in the pseudorapidity range $|\eta| < 2.5$, with the exception of the region $1.44 < |\eta| < 1.57$ where service infrastructure for the detector is located. They are identified using a multivariate-analysis (MVA) discriminator that combines observables sensitive to the amount of bremsstrahlung along the electron trajectory, the geometric and momentum matching between the electron trajectory and associated clusters, as well as various shower shape observables in the calorimeters. Electrons from photon conversions are removed. The chosen working point for selecting the electrons assures an average identification efficiency of 80% with a misidentification probability of 5%. The energy of electrons is determined from a combination of the track momentum at the primary vertex, the corresponding ECAL cluster energy, and the energy sum of all bremsstrahlung photons associated with the track.

Charged hadrons are identified as charged-particle tracks neither identified as electrons, nor as muons. Finally, neutral hadrons are identified as HCAL energy clusters not linked to any charged hadron trajectory, or as a combined ECAL and HCAL energy excess with respect to the expected charged hadron energy deposit. All the PF candidates are clustered into hadronic jets using the infrared- and collinear-safe anti-k_{T} algorithm [66], implemented in the FastJet package [70], with a distance parameter of 0.4. Jet momentum is determined as the vectorial sum of all particle momenta in the jet, and is found from simulation to be, on average, within 5 to 10% of the true momentum over the whole p_{T} spectrum and detector acceptance. Additional proton-proton interactions within the same or nearby bunch crossings can contribute additional tracks and calorimetric energy depositions, increasing the apparent jet momentum. To mitigate this effect, tracks identified to be originating from pileup vertices are discarded and an offset correction is applied to correct for remaining contributions. Jet energy corrections are derived from simulation studies so that the average measured response of jets becomes identical to that of particle level jets. In situ measurements of the momentum balance in dijet, photon+jet, Z+jets, and multijet events are used to determine any residual differences between the jet energy scale in data and in simulation, and appropriate corrections are made [71]. Additional selection criteria are applied to each jet to remove jets potentially dominated by instrumental effects or reconstruction failures.

JHEP03(2020)103

Hadronically decaying τ leptons (τ_h) are reconstructed and identified using the hadrons-plus-strips algorithm [72, 73]. The reconstruction starts from a jet and searches for the products of the main τ lepton decay modes: one charged hadron and up to two neutral pions, or three charged hadrons. To improve the reconstruction efficiency in the case of conversion of the photons from a neutral-pion decay, the algorithm considers the PF photons and electrons from a strip along ϕ. The sign of the τ_h candidate is determined through its decay products.

An MVA discriminator, based on variables such as lifetime information, decay mode, multiplicity of neutral, charged and pileup particles in a cone around the reconstructed τ_h, is used to reduce the rate for quark- and gluon-initiated jets identified as τ_h candidates. The working point used in the analysis is a "tight" one, with an efficiency of about 50% for a genuine τ_h, and approximately a 0.2% misidentification rate for quark and gluon jets [73]. Additionally, muons and electrons misidentified as τ_h are rejected by considering the consistency between the measurements in the tracker, calorimeters, and muon detectors. The specific identification criteria depend on the final state studied and on the background composition. The τ leptons that decay to muons and electrons are reconstructed in the same manner as prompt muons and electrons, respectively, as described above.

The variable $\Delta R = \sqrt{(\Delta\eta)^2 + (\Delta\phi)^2}$ is used to measure the separation between reconstructed objects in the detector, where η and ϕ are the pseudorapidity and azimuthal directions, respectively.

Jets misidentified as muons or electrons are suppressed by imposing isolation requirements. The muon (electron) isolation is measured relative to its p_T^ℓ ($\ell = \mu, e$) by summing over the p_T of PF particles in a cone with $\Delta R = 0.4$ (0.3) around the lepton, excluding the lepton itself:

$$I^\ell_{\text{rel}} = \frac{\sum p_T^{\text{charged}} + \max\left[0, \sum p_T^{\text{neutral}} + \sum p_T^{\gamma} - p_T^{\text{PU}}(\ell)\right]}{p_T^\ell},$$

where p_T^{charged}, p_T^{neutral}, and p_T^{γ} indicate the p_T of a charged and of a neutral particle, and a photon within the cone, respectively. The neutral particle contribution to isolation from pileup, $p_T^{\text{PU}}(\ell)$, is estimated from the p_T sum of charged hadrons not originating from the primary vertex scaled by a factor of 0.5 [68] for the muons. For the electrons, this contribution is estimated from the area of the jet and the average energy density of the event [74, 75]. The charged-particle contribution to isolation from pileup is rejected by requiring the tracks to originate from the primary vertex. Jet arising from a b quark are identified by the combined secondary vertex b tagging algorithm [76] using the working point characterised by a b jet identification efficiency around 65% and a misidentification probability around 1% for light quark and gluon jets.

All the reconstructed particles in the event are used to estimate the missing transverse momentum, $\vec{p}_T^{\text{miss}}$, which is defined as the projection onto the plane perpendicular to the beam axis of the negative vector sum of the momenta of all reconstructed PF candidates in an event [77]. The effect of the jet energy corrections described earlier in this section is then propagated to this $\vec{p}_T^{\text{miss}}$. The magnitude of the final vector is referred to as p_T^{miss}.

JHEP03(2020)103

The transverse mass $m_{\mathrm{T}}(\ell)$ is a variable formed from the lepton transverse momentum and the missing transverse momentum vectors: $m_{\mathrm{T}}(\ell) = \sqrt{2|\vec{p}_{\mathrm{T}}^{\,\ell}||\vec{p}_{\mathrm{T}}^{\,\mathrm{miss}}|(1-\cos\Delta\phi_{\ell-p_{\mathrm{T}}^{\mathrm{miss}}})}$, where $\Delta\phi_{\ell-p_{\mathrm{T}}^{\mathrm{miss}}}$ is the angle between the lepton transverse momentum and the missing transverse momentum. The collinear mass, M_{col}, provides an estimate of m_{H} using the observed decay products of the Higgs boson candidate. It is reconstructed using the collinear approximation based on the observation that, since $m_{\mathrm{H}} \gg m_{\tau}$, the τ lepton decay products are highly boosted in the direction of the τ candidate [78]. The neutrino momenta can be approximated to have the same direction as the other visible decay products of the τ lepton ($\vec{\tau}^{\,\mathrm{vis}}$) and the component of the $\vec{p}_{\mathrm{T}}^{\,\mathrm{miss}}$ in the direction of the visible τ lepton decay products is used to estimate the transverse component of the neutrino momentum ($p_{\mathrm{T}}^{\nu,\,\mathrm{est}}$). The collinear mass is then $M_{\mathrm{col}} = M_{\mathrm{vis}}/\sqrt{x_{\tau}^{\mathrm{vis}}}$, where x_{τ}^{vis} is the fraction of momentum carried by the visible decay products of the τ lepton, $x_{\tau}^{\mathrm{vis}} = p_{\mathrm{T}}^{\vec{\tau}^{\mathrm{vis}}}/(p_{\mathrm{T}}^{\vec{\tau}^{\mathrm{vis}}} + p_{\mathrm{T}}^{\nu,\,\mathrm{est}})$, and M_{vis} is the visible mass of the $\tau - \mathrm{e}$ or $\tau - \mu$ system.

Dedicated performance studies on data validate the reconstruction and identification techniques described in this section. When necessary, corrections have been applied to the simulated samples to ensure they correctly describe the behaviour of the data [68, 69, 71, 73, 76, 77].

5 Event selection

The event selection is performed in two steps. An initial selection is followed by another, final, set of requirements on kinematic variables that exploit the distinct event topology of the signal. The event sample defined by the initial selection is used in the background estimation described in section 6. The event selection begins by requiring two isolated leptons of opposite charge, different flavour, and separated by $\Delta R > 0.3$. The isolation of the τ_{h} candidates is included in the MVA discriminator described in section 4. Events with additional μ, e, or τ_{h} candidates respectively with $p_{\mathrm{T}} > 10$, 5, or 20 GeV are discarded. The kinematic requirements applied are dictated by the triggers or detector acceptance and are summarized in table 1.

The events are then divided into two categories according to the number of jets in the event. The jets are required to have $p_{\mathrm{T}} > 30$ GeV and $|\eta| < 4.7$. Events with no jets form the 0-jet category while events with exactly one jet form the 1-jet category. The 1-jet category includes ggH production with initial state radiation. Events with more than one jet are discarded.

The final selection is given in table 2. It begins by tightening the p_{T} requirement of the prompt lepton from the Higgs boson decay, as it provides a powerful discriminant against the background. The τ lepton in the H decay is highly boosted, leading to a collimation of the decay products. This can be exploited by either limiting the azimuthal separation of the decay products including the $\vec{p}_{\mathrm{T}}^{\,\mathrm{miss}}$, or imposing a requirement on the transverse mass $m_{\mathrm{T}}(\tau)$, which is strongly correlated with the azimuthal separation. These selection criteria are optimised for each decay mode in two m_{H} ranges to obtain the most stringent expected upper limits. The low- and high-mass regions are defined to be $200 < m_{\mathrm{H}} < 450$ GeV and

JHEP03(2020)103

	$H \to \mu\tau_h$	$H \to \mu\tau_e$	$H \to e\tau_h$	$H \to e\tau_\mu$
p_T^μ	>53 GeV	>53 GeV	—	>10 GeV
p_T^e	—	>10 GeV	>26 GeV	>26 GeV
p_T^τ	>30 GeV	—	>30 GeV	—
$\lvert\eta^\mu\rvert$	<2.4	<2.4	—	<2.4
$\lvert\eta^e\rvert$	—	<2.4	<2.1	<2.4
$\lvert\eta^\tau\rvert$	<2.3	—	<2.3	—
I^μ_{rel}	0.15	<0.15	—	<0.15
I^e_{rel}	—	<0.1	<0.1	<0.1
$\Delta R(\mu, e)$	—	>0.3	—	>0.3
$\Delta R(\mu, \tau)$	>0.3	—	—	—
$\Delta R(e, \tau)$	—	—	>0.3	—

Table 1. Initial selection criteria applied to the kinematic variables for the $H \to \mu\tau$ and $H \to e\tau$ analyses. The selected sample is used in the background estimation from control samples in data.

$450 < m_H < 900\,\text{GeV}$, respectively. A binned likelihood fit to the M_{col} distributions is then used to extract signal and background contributions. The M_{col} approximates the Higgs mass better than the widely used M_{vis}, and therefore improves the separation of the signal from the background. This improvement is larger in the high mass regime, with up to a factor of three gain in sensitivity when compared to the use of M_{vis}.

6 Background estimation

The most significant background in the $\mu\tau_h$ and $e\tau_h$ channels comes from the W+jets process and from events comprised uniquely of jets produced through the strong interaction, referred to as quantum chromodynamics (QCD) multijet events. In these processes, jets are misidentified as electrons, muons or τ leptons. This background is estimated with the collected data. The main background in the $\mu\tau_e$ and $e\tau_\mu$ channels is $t\bar{t}$ production. It is estimated using simulations. Other smaller backgrounds include electroweak diboson (WW, WZ, and ZZ), Drell-Yan (DY)$\to \ell\ell$ ($\ell = e, \mu$) + jets, DY$\to \tau\tau$ + jets, SM Higgs boson ($H \to \tau\tau, WW$), W$\gamma^{(*)}$+jets, and single top quark production processes. These are estimated using simulations. Gluon fusion, vector boson fusion, and associated production mechanisms are considered for the SM Higgs boson background. The background estimation techniques are described in detail below, and are validated with control regions that are enhanced with the dominant backgrounds.

The DY$\to \ell\ell, \tau\tau$ background is estimated from simulation. A reweighting is applied to the generator-level Z boson p_T and invariant mass, $m_{\ell\ell,\tau\tau}$, distributions to correct for a shape discrepancy between data and simulation. The reweighting factors, extracted from a control region enriched in $Z \to \mu\mu$ events, are applied in bins of Z boson p_T and $m_{\ell\ell,\tau\tau}$ as explained in [45]. Additional corrections for $e \to \tau_h$ and $\mu \to \tau_h$ misidentification rates are

JHEP03(2020)103

		Low-mass range	High-mass range
$H \to \mu\tau_h$	0-jet	$p_T^\mu > 60\,GeV$	$p_T^\mu > 150\,GeV$
		$p_T^\tau > 30\,GeV$	$p_T^\tau > 45\,GeV$
		$m_T(\tau_h) < 105\,GeV$	$m_T(\tau_h) < 200\,GeV$
	1-jet	$p_T^\mu > 60\,GeV$	$p_T^\mu > 150\,GeV$
		$p_T^\tau > 30\,GeV$	$p_T^\tau > 45\,GeV$
		$m_T(\tau_h) < 120\,GeV$	$m_T(\tau_h) < 230\,GeV$
$H \to \mu\tau_e$	0-jet	$p_T^\mu > 60\,GeV$	$p_T^\mu > 150\,GeV$
		$p_T^e > 10\,GeV$	$p_T^e > 10\,GeV$
		$\Delta\phi(e, \vec{p}_T^{\,miss}) < 0.7\,rad$	$\Delta\phi(e, \vec{p}_T^{\,miss}) < 0.3\,rad$
		$\Delta\phi(e, \mu) > 2.2\,rad$	$\Delta\phi(e, \mu) > 2.2\,rad$
	1-jet	$p_T^\mu > 60\,GeV$	$p_T^\mu > 150\,GeV$
		$p_T^e > 10\,GeV$	$p_T^e > 10\,GeV$
		$\Delta\phi(e, \vec{p}_T^{\,miss}) < 0.7\,rad$	$\Delta\phi(e, \vec{p}_T^{\,miss}) < 0.3\,rad$
		$\Delta\phi(e, \mu) > 2.2\,rad$	$\Delta\phi(e, \mu) > 2.2\,rad$
$H \to e\tau_h$	0-jet	$p_T^e > 60\,GeV$	$p_T^e > 150\,GeV$
		$p_T^\tau > 30\,GeV$	$p_T^\tau > 45\,GeV$
		$m_T(\tau_h) < 105\,GeV$	$m_T(\tau_h) < 200\,GeV$
	1-jet	$p_T^e > 60\,GeV$	$p_T^e > 150\,GeV$
		$p_T^\tau > 30\,GeV$	$p_T^\tau > 45\,GeV$
		$m_T(\tau_h) < 120\,GeV$	$m_T(\tau_h) < 230\,GeV$
$H \to e\tau_\mu$	0-jet	$p_T^e > 60\,GeV$	$p_T^e > 150\,GeV$
		$p_T^\mu > 10\,GeV$	$p_T^\mu > 10\,GeV$
		$\Delta\phi(\mu, \vec{p}_T^{\,miss}) < 0.7\,rad$	$\Delta\phi(\mu, \vec{p}_T^{\,miss}) < 0.3\,rad$
		$\Delta\phi(e, \mu) > 2.2\,rad$	$\Delta\phi(e, \mu) > 2.2\,rad$
	1-jet	$p_T^e > 60\,GeV$	$p_T^e > 150\,GeV$
		$p_T^\mu > 10\,GeV$	$p_T^\mu > 10\,GeV$
		$\Delta\phi(\mu, \vec{p}_T^{\,miss}) < 0.7\,rad$	$\Delta\phi(\mu, \vec{p}_T^{\,miss}) < 0.3\,rad$
		$\Delta\phi(e, \mu) > 2.2\,rad$	$\Delta\phi(e, \mu) > 2.2\,rad$

Table 2. Final event selection criteria for the low-mass range, $200 < m_H < 450\,GeV$, and the high-mass range, $450 < m_H < 900\,GeV$, considered in the $H \to \mu\tau$ and $H \to e\tau$ analyses.

JHEP03(2020)103

applied to the simulated DY sample when the reconstructed τ_h candidate is matched to an electron for the $H \to e\tau_h$ channel or a muon for the $H \to \mu\tau_h$ channel, respectively, at the generator level. These corrections depend on the lepton η and are measured in $Z \to \ell\ell$ data events.

The $t\bar{t}$ background is also estimated using simulation. The overall normalisation of this estimate in the signal region is corrected with a rescaling factor derived from a control region enriched in $t\bar{t}$ events, defined by requiring the initial selection with the additional requirement that at least one of the jets is b tagged. Figure 1 (upper left) shows the data compared to the background estimate in the $t\bar{t}$-enriched region in the $H \to \mu\tau_e$ channel.

Jets from W+jets and QCD multijet events that are misidentified as electrons, muons and, mainly, τ leptons, are leading source of background in the $\mu\tau_h$ and $e\tau_h$ channels. In W+jets events, one lepton candidate is expected to be a genuine lepton from the W decay and the other a jet misidentified as a lepton. In QCD multijet events, both lepton candidates are misidentified jets. A technique fully based on control samples in data is used to estimate the misidentified lepton background in the $\mu\tau_h$ and $e\tau_h$ channels, for which it is the dominant contribution. In the $\mu\tau_e$ and $e\tau_\mu$ channels, this background is estimated using a combination of simulated samples and control regions in data. These methods have been used in refs. [38] and [45], and a detailed description can be found in those publications. However, we are briefly describing the techniques in the following subsections.

6.1 Misidentified lepton background estimation from control samples in data

The misidentified-lepton background is estimated from data. The misidentification probabilities, f_i, where $i = \mu$, e, or τ_h, are evaluated with independent Z+jets data sets and then applied to a control sample. The control sample is obtained by relaxing the signal selection requirements, the μ, e, or τ_h isolation, and excluding events passing the signal selection. The f_i are estimated using events with a Z boson candidate and one jet that can be misidentified as μ, e, or τ. The Z boson candidate is formed requiring two muons with $p_T > 26\,\text{GeV}$, $|\eta| < 2.4$, and $I^{\mu}_{\text{rel}} < 0.15$. The muons are required to have opposite charges and the dimuon invariant mass, $m_{\mu\mu}$, must satisfy $76 < m_{\mu\mu} < 106\,\text{GeV}$. The contribution from diboson events, where the third lepton candidate corresponds to a genuine μ, e, or τ, is subtracted using simulation. Two Z+jets samples are defined: a signal-like one, in which the jet satisfies the same μ, e, or τ selection criteria used in the $H \to \mu\tau$ or $H \to e\tau$ selections, and a background-enriched Z+jets sample with relaxed identification on the jet misidentified as μ, e, or τ, but excluding events selected in the signal-like sample. The requirements on the third candidate, i.e. the misidentified jet, depend on the lepton flavour. The two samples are used to estimate f_i as

$$f_i = \frac{N_i(\text{Z+jets signal-like})}{N_i(\text{Z+jets background-enriched}) + N_i(\text{Z+jets signal-like})},$$

where N_i(Z+jets signal-like) is the number of events with a third candidate (μ, e, or τ) that passes the signal-like sample selection, and N_i(Z+jets background-enriched) is the number of events in the background-enriched sample. The background-enriched selection used to estimate the misidentified μ and e contribution requires an isolation of $0.15 < I^{\mu}_{\text{rel}} < 0.25$

JHEP03(2020)103

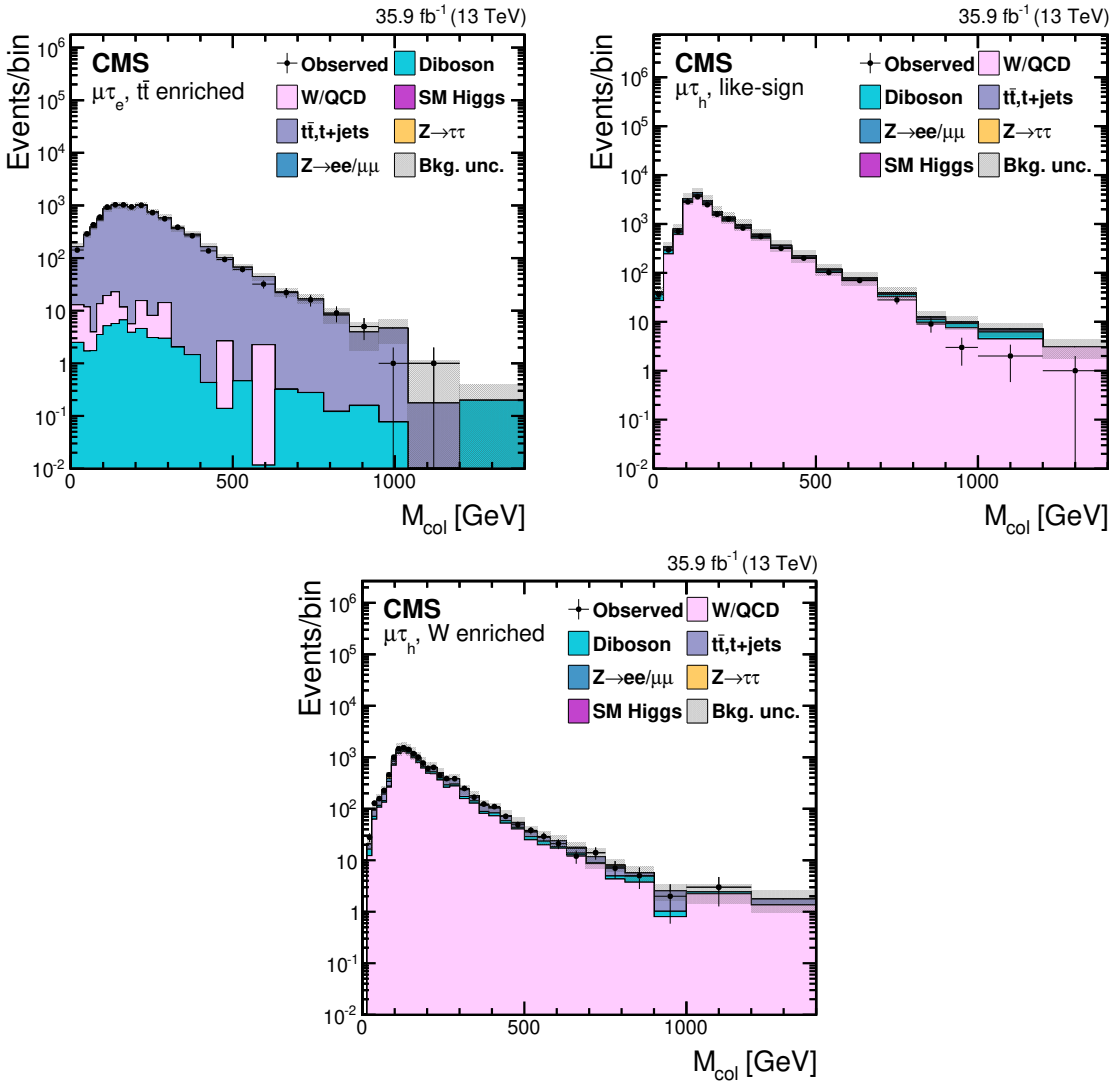

Figure 1. The M_{col} distribution in the $\mathrm{t\bar{t}}$ enriched (upper left), like-sign lepton (upper right), and W+jets enriched (lower) control samples defined in the text. The uncertainty bands include both statistical and systematic uncertainties from section 7. No fit is performed for these distributions. The different background processes shown are normalised to the luminosity of the data either using the theoretical prediction of the corresponding production cross section or directly from the data driven technique described in the text.

and $0.1 < I^{\text{e}}_{\text{rel}} < 0.5$, respectively. In both cases the misidentification rate is computed and applied as a function of the lepton p_{T}. The lepton selection for the τ_{h} background-enriched sample requires that the τ_{h} lepton candidates are identified using a loose τ_{h} identification and isolation working point but are not identified by the tight working point used for the signal selection. The loose and tight working points have an efficiencies of 70 and 50% for genuine τ_{h} candidates, respectively.

The τ_{h} misidentification rates have a p_{T} dependence that varies with the number of charged pions in the decay. They are estimated and applied as a function of p_{T} and for

JHEP03(2020)103

either one or three charged pions in the decay. The misidentified background in the signal sample is obtained from control samples for each lepton flavour. The selection requirements for these samples are the same as for the signal sample except that the μ, e, or τ should pass the identification and isolation criteria used for the Z+jets background-enriched sample, but not those defining the Z+jets signal-like sample. To estimate the misidentified background in the signal sample, each event in this background enriched sample is weighted by a factor $f_i/(1-f_i)$. The background from misidentified muons and electrons is estimated to be less than 5% of the misidentified τ_h lepton background and is neglected.

The background estimate is validated in a like-sign sample by applying the misidentification rate f_i to events selected by requiring the μ, e, or τ in the pairs having the same charge in both the background-enriched and the signal-like samples. This validation is performed after the initial selection described in section 5. Figure 1 (upper right) shows the data compared to the background estimate in the like-sign control region for the $H \to \mu\tau_h$ channel. The like-sign selection enhances the misidentified-lepton background, and this sample is expected to be composed of a similar fraction of W+jets and QCD multijet events. The background estimate is also validated in a W boson enriched control sample. This data sample is obtained by applying the signal sample requirements and m_T cuts, $50 < m_T(\ell) < 110\,\text{GeV}$ ($\ell = \mu$ or e) and $m_T(\tau) > 50\,\text{GeV}$. The misidentified background in the signal region and W boson enriched control sample are both dominated by W+jets events, with QCD multijet events forming a small fraction of the samples. Figure 1 (lower) shows the data compared to the background estimate in the W+jets enriched sample for the $H \to \mu\tau_h$ channel. The background expectation for the $H \to e\tau_h$ channel is also validated with the same samples and gives similar agreement.

6.2 W+jets and QCD background estimation in $\mu\tau_e$ and $e\tau_\mu$ channels

The W+jets background contribution to the misidentified background is estimated with simulations. The QCD multijet contribution is estimated with like-sign data events that pass all the other signal requirements. The remaining non-QCD background is estimated using simulation. The resulting sample is then rescaled to account for the differences between the background composition in the like and opposite sign samples. The scaling factors are extracted from QCD multijet enriched control samples, composed of events where the lepton candidates satisfy inverted isolation requirements, as explained in ref. [45]. This background contribution accounts for a negligible fraction of the total yield after selection in both $\mu\tau_e$ and $e\tau_\mu$ channels.

7 Systematic uncertainties

Systematic uncertainties arise from both experimental and theoretical sources and can affect the normalisation and the shape of the collinear mass distribution. They are summarized in table 3.

The uncertainties in the muon, electron and τ lepton selection including the trigger, identification (ID), and isolation efficiencies are estimated from collision data sets of Z bosons decaying to $ee, \mu\mu, \tau_\mu\tau_h$ [68, 69, 73]. They result in changes of normalisation, with

JHEP03(2020)103

Systematic uncertainty	$H \to \mu\tau_h$	$H \to \mu\tau_e$	$H \to e\tau_h$	$H \to e\tau_\mu$
Muon trigger/ID/isolation	2%	2%	—	2%
Electron trigger/ID/isolation	—	2%	2%	2%
Hadronic τ_h efficiency	5%	—	5%	—
High p_T τ_h efficiency	$^{+5}_{-35}\% \times p_T \times 0.001$	—	$^{+5}_{-35}\% \times p_T \times 0.001$	—
b tagging veto	2.0–2.5%	2.0–2.5%	2.0–2.5%	2.0–2.5%
$\mu \to \tau_h$ background	25%	—	—	—
$e \to \tau_h$ background	—	—	12%	—
jet $\to \tau_h$ background	30%⊕10%	—	30%⊕10%	—
QCD multijet background	—	30%	—	30%
$Z \to \mu\mu/ee$ + jets background	—	0.1%⊕2%⊕5%	—	0.1%⊕2%⊕5%
$Z \to \tau\tau$ + jets background	0.1%⊕2%⊕5%	0.1%⊕2%⊕5%	0.1%⊕2%⊕5%	0.1%⊕2%⊕5%
W+jets background	—	0.8%⊕3.8%⊕5%	—	0.8%⊕3.8%⊕5%
WW, ZZ, WZ background	3.5%⊕5%⊕5%	3.5%⊕5%⊕5%	3.5%⊕5%⊕5%	3.5%⊕5%⊕5%
W+γ background	—	10%⊕5%	—	10%⊕5%
Single top quark background	3%⊕5%⊕5%	3%⊕5%⊕5%	3%⊕5%⊕5%	3%⊕5%⊕5%
$t\bar{t}$ background	10%⊕5%	10%⊕5%	10%⊕5%	10%⊕5%
SM Higgs fact./renorm. scales	3.9 %	3.9 %	3.9 %	3.9 %
SM Higgs PDF+α_S	3.2 %	3.2 %	3.2 %	3.2 %
Jet energy scale	3–20%	3–20%	3–20%	3–20%
τ_h energy scale	1.2%	—	1.2%	—
$\mu, e \to \tau_h$ energy scale	1.5%	—	3%	—
μ energy scale	0.2%	0.2%	—	0.2%
e energy scale	—	0.1–0.5%	0.1–0.5%	0.1–0.5%
Unclustered energy scale	$\pm 1\sigma$	$\pm 1\sigma$	$\pm 1\sigma$	$\pm 1\sigma$
IntegRated luminosity	2.5%	2.5%	2.5%	2.5%

Table 3. The systematic uncertainties for the four channels. All uncertainties are treated as correlated between the categories, except those with more values separated by the ⊕ symbol. In the case of two values, the first value is the correlated uncertainty and the second value is the uncorrelated uncertainty for each individual category. In the case of three values, the first and second values correspond to the uncertainties arising from factorisation and renormalisation scales and PDF variations and are correlated between categories, while the third value is the uncorrelated uncertainty for each individual category. Two values separated by the "–" sign represent the range of the uncertainties from the different sources and/or in the different jet categories.

JHEP03(2020)103

m_{H} (GeV)	Cross section (pb)	Theory, Gaussian (%)	PDF+α_S (%)
200	16.94	±1.8	±3.0
300	6.59	±1.8	±3.0
450	2.30	±2.0	±3.1
600	1	±2.1	±3.5
750	0.50	±2.1	±4.0
900	0.27	±2.2	±4.6

Table 4. Theoretical uncertainties from [79] are applied to the Higgs boson production cross sections for the different masses. In the reference, the PDF and α_S uncertainties are computed following the recommendation of the PDF4LHC working group. The remaining Gaussian uncertainty accounts for additional intrinsic sources of theory uncertainty described in detail in the reference.

the exception of the uncertainty on high p_{T} τ lepton efficiency that changes both yield and M_{col} distribution shape. The b tagging efficiency is measured in collision data, and the simulation is adjusted accordingly to match with it. The uncertainty in this measurement is taken as the systematic error affecting the normalisation of the simulation [76].

The uncertainties in the estimate of the misidentified-lepton backgrounds ($\mu \to \tau_{\mathrm{h}}$, $\mathrm{e} \to \tau_{\mathrm{h}}$, jet $\to \tau_{\mathrm{h}}, \mu, \mathrm{e}$) are extracted from the validation tests in control samples, as described in section 6; they affect both the normalisation and the shape of the M_{col} distribution. The uncertainty in the QCD multijet background yield is 30%, and corresponds to the uncertainty in the extrapolation factor from the same-sign to the opposite-sign region, as determined in ref. [45]. The uncertainties in the background contributions from Z, WW, ZZ, $\mathrm{W}\gamma$, $\mathrm{t\bar{t}}$ and single-top quark arise predominantly from those in the measured cross sections of these processes and are applied as uncertainties in sample normalisation.

The uncertainties in the Higgs boson production cross sections due to the factorisation and the renormalisation scales, as well as the PDFs and the strong coupling constant (α_S), result in changes in normalisation. They are taken from ref. [79] and summarized in table 3 for the SM Higgs boson and table 4 for heavy Higgs bosons. Only effects on the total rate are considered. Effects on the acceptance have been neglected.

Shape and normalization uncertainties arising from the uncertainty in the jet energy scale are computed by propagating the effect of altering each source of jet energy scale uncertainty by ±1 standard deviation to the fit templates of each process. There are 27 independent sources of jet energy scale uncertainty, fully correlated between categories and τ lepton decay channels.

The uncertainty in the τ_{h} energy scale is treated equally for the two independent channels: $\mathrm{H} \to \mu\tau_h$ and $\mathrm{H} \to \mathrm{e}\tau_h$. It is propagated to the collinear mass distributions. Also, the uncertainty in the energy scale of electrons and muons misidentified as τ_{h} is propagated to the M_{col} distributions and produces changes in the distribution shape and normalization. Systematic uncertainties in the electron energy scale and resolution include the effects of electron selection efficiency, pseudorapidity dependence and categorisation, summed in quadrature. They impact both the normalization and shape of the M_{col} distribution. The

JHEP03(2020)103

systematic uncertainties in the energy resolution have negligible effect. The uncertainty in muon energy scale and resolution is also treated in the same manner. Scale uncertainties on the energy from jets with p_T below 15 GeV and PF candidates not clustered inside jets (unclustered energy scale uncertainty) are also considered [77]. They are estimated independently for four particle categories: charged particles, photons, neutral hadrons, and very forward particles which are not contained in jets. The effect of shifting the energy of each particle by its uncertainty is propagated to p_T^{miss} and leads to both changes in shape of the distribution and in overall predicted yields. The different systematic uncertainties from the four particle categories, for the unclustered energy scale, are considered uncorrelated.

The bin-by-bin uncertainties [80] account for the statistical uncertainties in every bin of the template distributions of every process. They are uncorrelated between bins, processes, and categories.

Shape uncertainties related to the pileup have been considered by varying the weights applied to simulation. This weight variation is obtained changing by 5% the total inelastic cross section used in the estimate of the pileup events in data [81]. The new values are then applied, event by event, to produce alternative collinear mass distributions used as shape uncertainties in the fit. Other minimum bias event modelling and simulation uncertainties are estimated to be much smaller and are therefore neglected. The uncertainty on the integrated luminosity affects all processes with normalization taken directly from simulation.

8 Results

After all selection criteria have been applied, a binned maximum likelihood fit is performed on the M_{col} distributions in the range 0–1400 GeV, looking for a signal-like excess on top of the estimated background. No fit on the control region is performed. The systematic uncertainties are represented by nuisance parameters, assuming a log normal prior for normalisation parameters, and Gaussian priors for M_{col} shape uncertainties. The uncertainties that affect the shape of the M_{col} distribution, mainly those corresponding to the energy scales, are represented by nuisance parameters whose variation results in a modification of the distribution [82, 83]. A profile likelihood ratio is used as test statistic. The 95% CL upper limits on the H production cross section times branching fraction to LFV lepton channels, $\sigma(gg \to H)\mathcal{B}(H \to \mu\tau)$ and $\sigma(gg \to H)\mathcal{B}(H \to e\tau)$, are set using the CL_s criterion [84, 85] and the asymptotic approximation of the distributions of the LHC test-statistic [86], in a combined fit to the M_{col} distributions. The limits are also computed per channel and category. The upper limits are derived in the analysed mass range in steps of 50 GeV. Where simulated samples are not available, shapes and yields are interpolated from the neighbouring samples with a moment morphing algorithm that derive the M_{col} distribution from the two closest simulated mass points.

8.1 $H \to \mu\tau$ results

The distributions of the collinear mass M_{col} compared to the signal and background contributions in the $H \to \mu\tau_h$ and $H \to \mu\tau_e$ channels, in each jet category, are shown in figures 2 and 3. No excess over the background expectation is observed. The observed and

JHEP03(2020)103

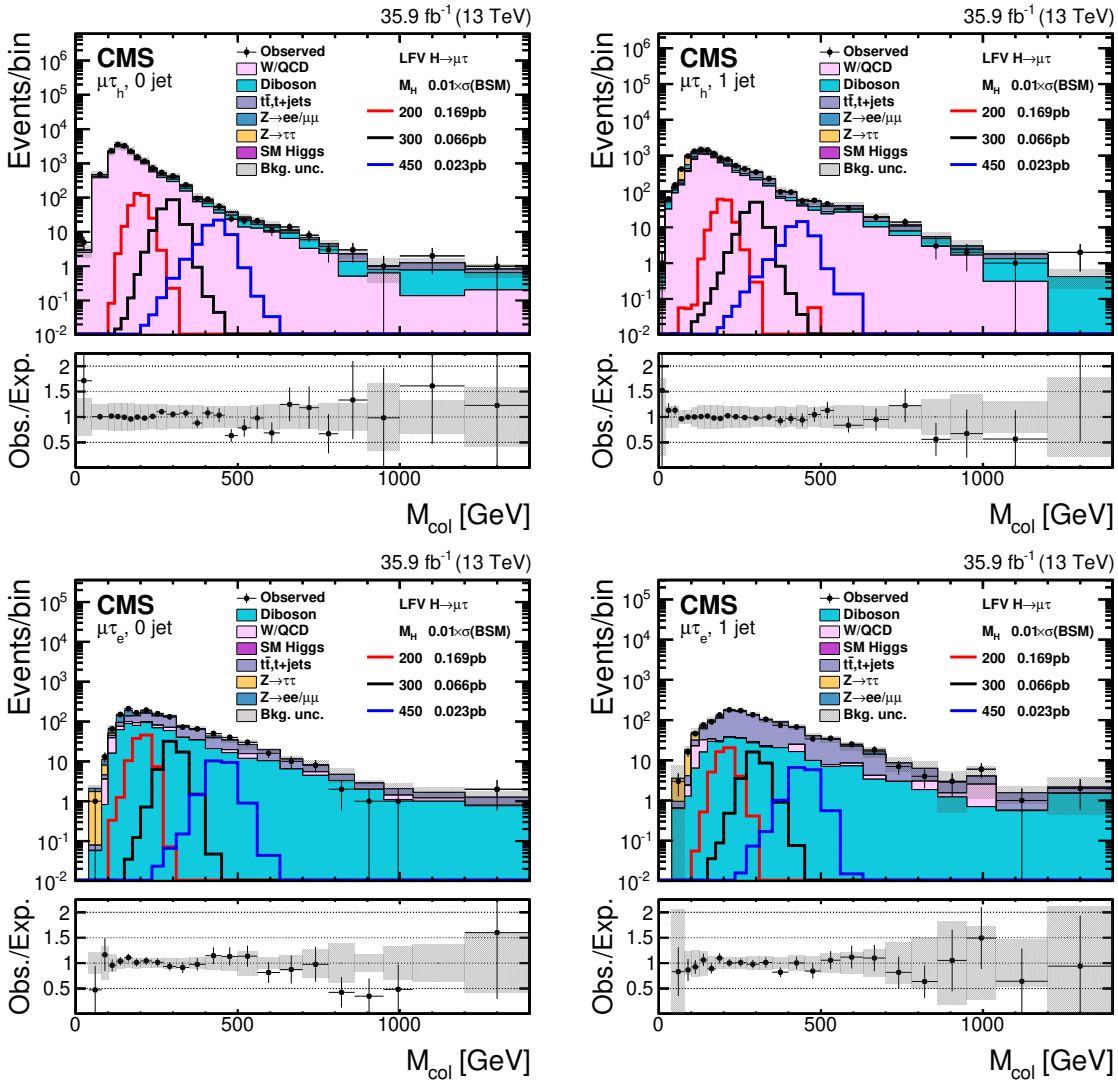

Figure 2. The M_{col} distribution in the signal region, for the $\mu\tau_{\text{h}}$ (upper) and $\mu\tau_{\text{e}}$ (lower) channels for the Higgs boson mass in the range 200–450 GeV for 0-jet (left) and 1-jet (right) categories. The uncertainty bands include both statistical and systematic uncertainties. The plotted values are number of events per bin using a variable bin size. The background is normalised to the best fit values from a binned likelihood fit, discussed in the text, to the background only hypothesis. For depicting the signals a branching fraction of 1% and BSM cross sections from ref. [79] are assumed.

median expected 95% CL upper limits on $\sigma(\text{gg} \to \text{H})\mathcal{B}(\text{H} \to \mu\tau)$ range from 51.9 (57.4) fb to 1.6 (2.1) fb, and are given for each category in table 5.The limits are also summarized graphically in figure 4 for the individual categories, and in figure 5 for the combination of the two τ decay channels.

JHEP03(2020)103

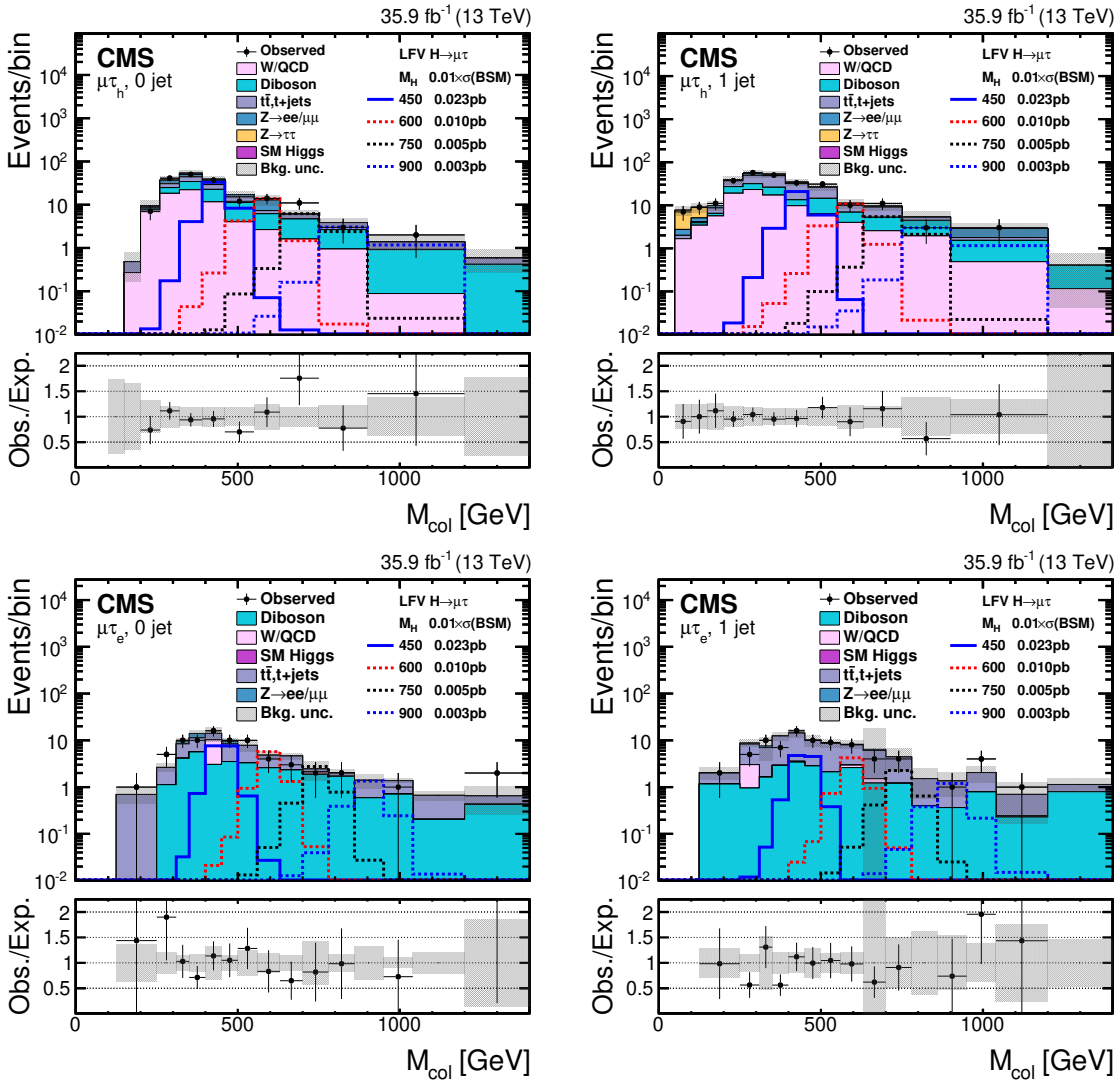

Figure 3. The M_{col} distribution in the signal region, for the $\mu\tau_{\mathrm{h}}$ (upper) and $\mu\tau_{\mathrm{e}}$ (lower) channels for the Higgs boson mass in the range 450–900 GeV for 0-jet (left) and 1-jet (right) categories. The uncertainty bands include both statistical and systematic uncertainties. The plotted values are number of events per bin using a variable bin size. The background is normalised to the best fit values from a binned likelihood fit, discussed in the text, to the background only hypothesis. For depicting the signals a branching fraction of 1% and BSM cross sections from ref. [79] are assumed.

JHEP03(2020)103

Observed 95% CL upper limit on $\sigma(gg \to H)\mathcal{B}(H \to \mu\tau)$ (fb)									
	$\mu\tau_e$			$\mu\tau_h$			$\mu\tau$		
m_H (GeV)	0 jet	1 jet	comb	0 jet	1 jet	comb	0 jet	1 jet	comb
200	147.8	262.1	159.4	53.1	136.9	46.4	53.3	133.9	51.9
300	30.1	100.8	29.3	57.4	49.4	51.4	33.2	45.5	32.7
450	31.1	35.3	23.7	9.1	14.2	7.3	14.7	14.6	8.1
600	8.1	15.2	6.8	7.5	7.4	5.3	9.1	6.5	4.1
750	6.5	7.8	4.7	4.8	4.8	3.2	3.6	3.7	2.5
900	4.4	5.6	2.9	4.6	2.6	2.3	3.0	2.1	1.6

Median expected 95% CL upper limit on $\sigma(gg \to H)\mathcal{B}(H \to \mu\tau)$ (fb)									
	$\mu\tau_e$			$\mu\tau_h$			$\mu\tau$		
m_H (GeV)	0 jet	1 jet	comb	0 jet	1 jet	comb	0 jet	1 jet	comb
200	107.5	209.8	95.6	79.7	151.6	72.5	63.7	126.1	57.4
300	49.8	108.6	45.2	31.0	54.8	27.7	25.9	48.8	23.4
450	17.5	32.8	20.4	9.4	15.3	8.0	8.2	13.6	7.7
600	10.4	17.9	8.9	6.2	8.3	4.9	5.1	7.4	4.2
750	8.0	11.1	6.1	4.3	5.4	3.1	3.6	4.7	2.7
900	6.9	8.0	4.9	3.3	4.3	2.4	2.8	3.5	2.1

Table 5. The observed and median expected 95% CL upper limits on $\sigma(gg \to H)\mathcal{B}(H \to \mu\tau)$.

8.2 $H \to e\tau$ results

The distributions of the collinear mass M_{col} compared to the signal and background contributions in the $H \to e\tau_h$ and $H \to e\tau_\mu$ channels, in each category, are shown in figures 6 and 7. No excess over the background expectation is observed. The observed and median expected 95% CL upper limits on $\sigma(gg \to H)\mathcal{B}(H \to e\tau)$ range from 94.1 (91.6) fb to 2.3 (2.3) fb, and are given for each category in table 6. The limits are also summarized graphically in figure 8 for the individual categories, and in figure 9 for the combination of both two τ decay channels.

9 Summary

The first direct search for lepton flavour violating decays of a neutral non-standard-model Higgs boson (H) in the $\mu\tau$ and $e\tau$ channels is presented in this paper. The analyzed data set corresponds to an integrated luminosity of 35.9 fb^{-1} of proton-proton collision data recorded at $\sqrt{s} = 13$ TeV. The results are extracted from a fit to the collinear mass distributions. No evidence is found for lepton flavour violating decays of H in the investigated mass range. The observed (expected) upper limits at 95% confidence level on the product of production

JHEP03(2020)103

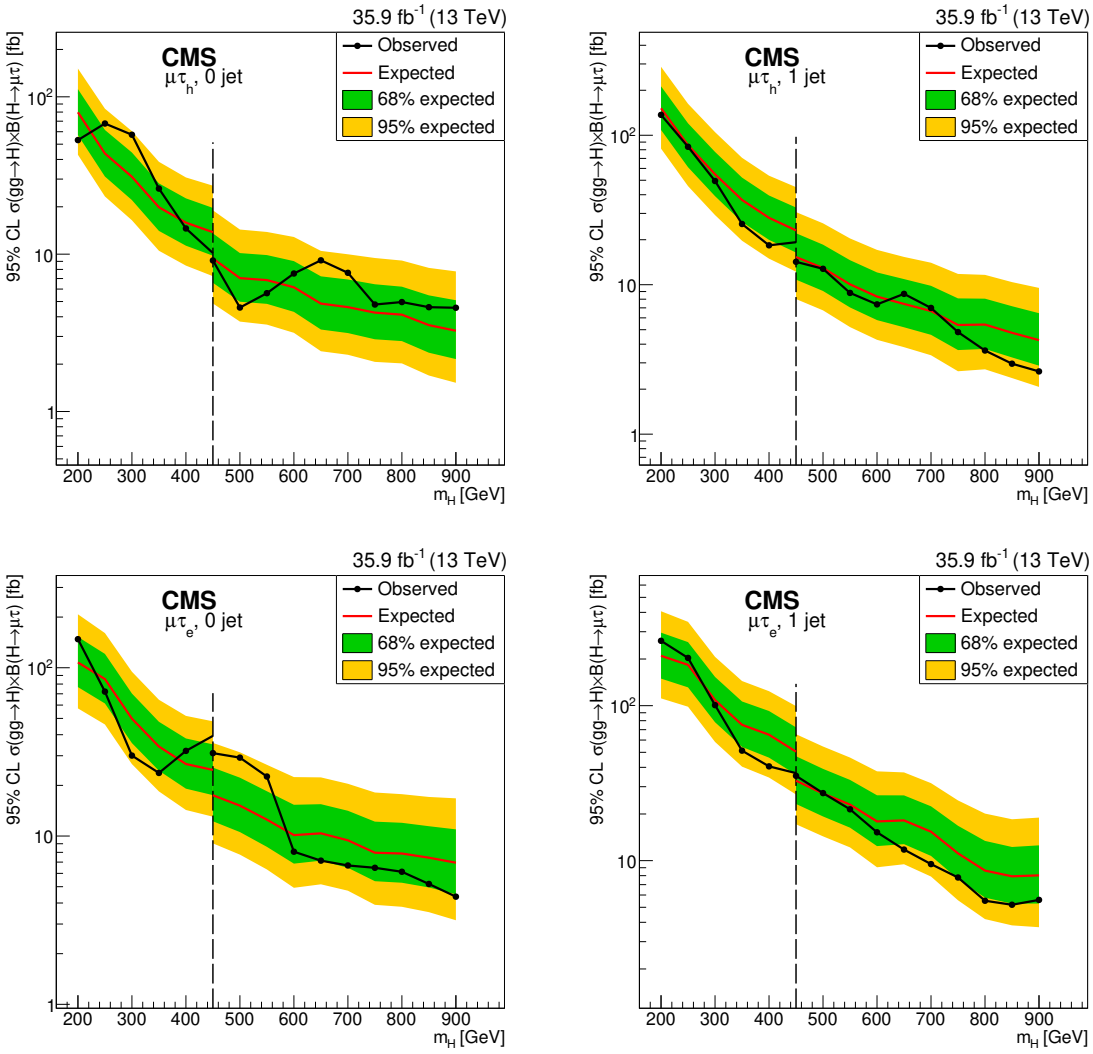

Figure 4. The observed and median expected 95% CL upper limits on $\sigma(gg \to H)\mathcal{B}(H \to \mu\tau)$, for the $\mu\tau_h$ (upper) and $\mu\tau_e$ (lower) channels, for 0-jet (left) and 1-jet (right) categories. The dashed line shows the transition between the two investigated mass ranges.

cross section with branching fraction, for H mass in the range 200–900 GeV, decaying to $\mu\tau$ and $e\tau$ vary from 51.9 (57.4) fb to 1.6 (2.1) fb and from 94.1 (91.6) fb to 2.3 (2.3) fb, respectively.

Acknowledgments

We congratulate our colleagues in the CERN accelerator departments for the excellent performance of the LHC and thank the technical and administrative staffs at CERN and at other CMS institutes for their contributions to the success of the CMS effort. In addition, we gratefully acknowledge the computing centres and personnel of the Worldwide LHC Computing Grid for delivering so effectively the computing infrastructure essential to our

JHEP03(2020)103

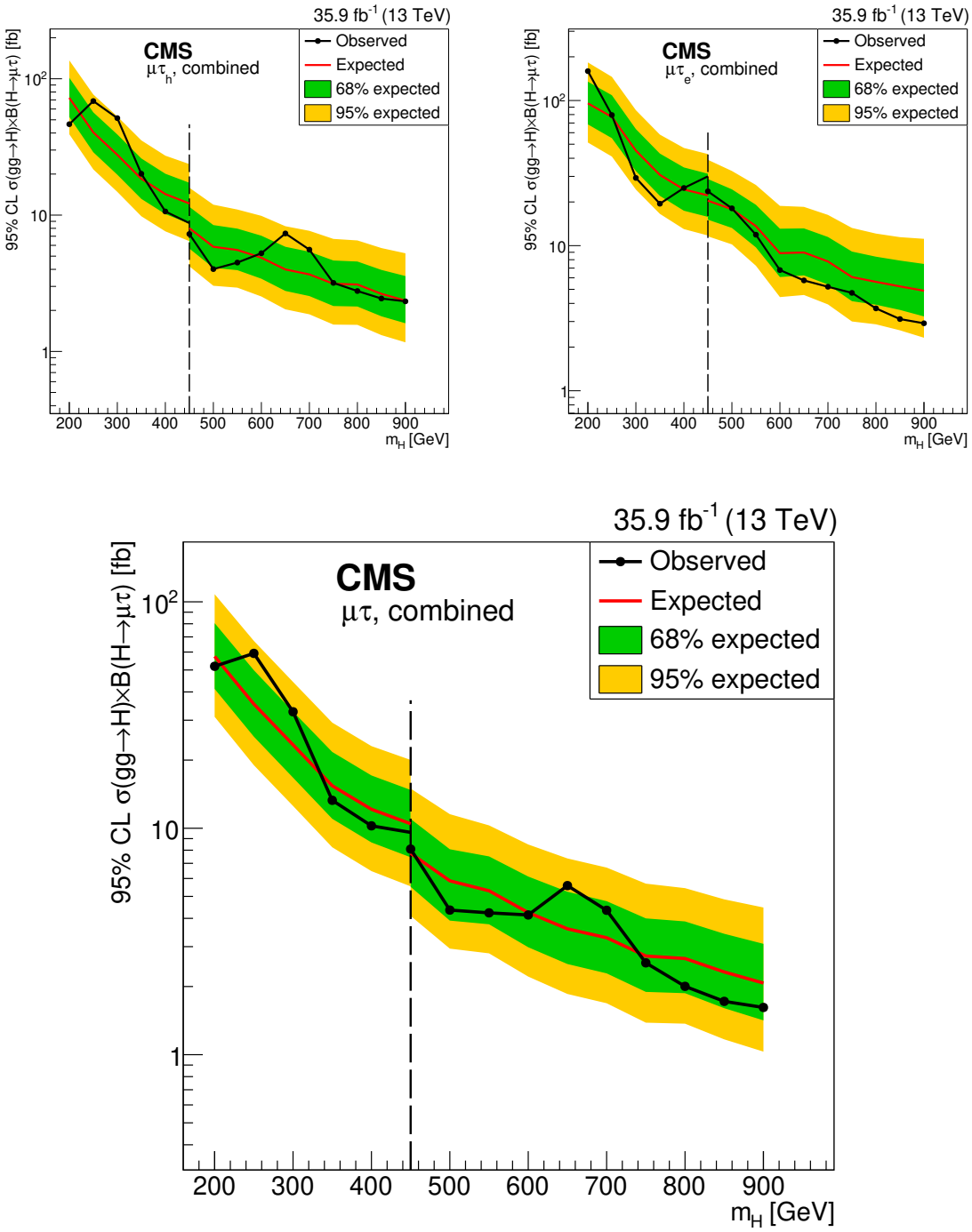

Figure 5. The combined observed and median expected 95% CL upper limits on $\sigma(gg \to H)\mathcal{B}(H \to \mu\tau)$, for $\mu\tau_h$ (upper left) and $\mu\tau_e$ (lower right) channels, and their combination $\mu\tau$ (lower). The dashed line shows the transition between the two investigated mass ranges.

JHEP03(2020)103

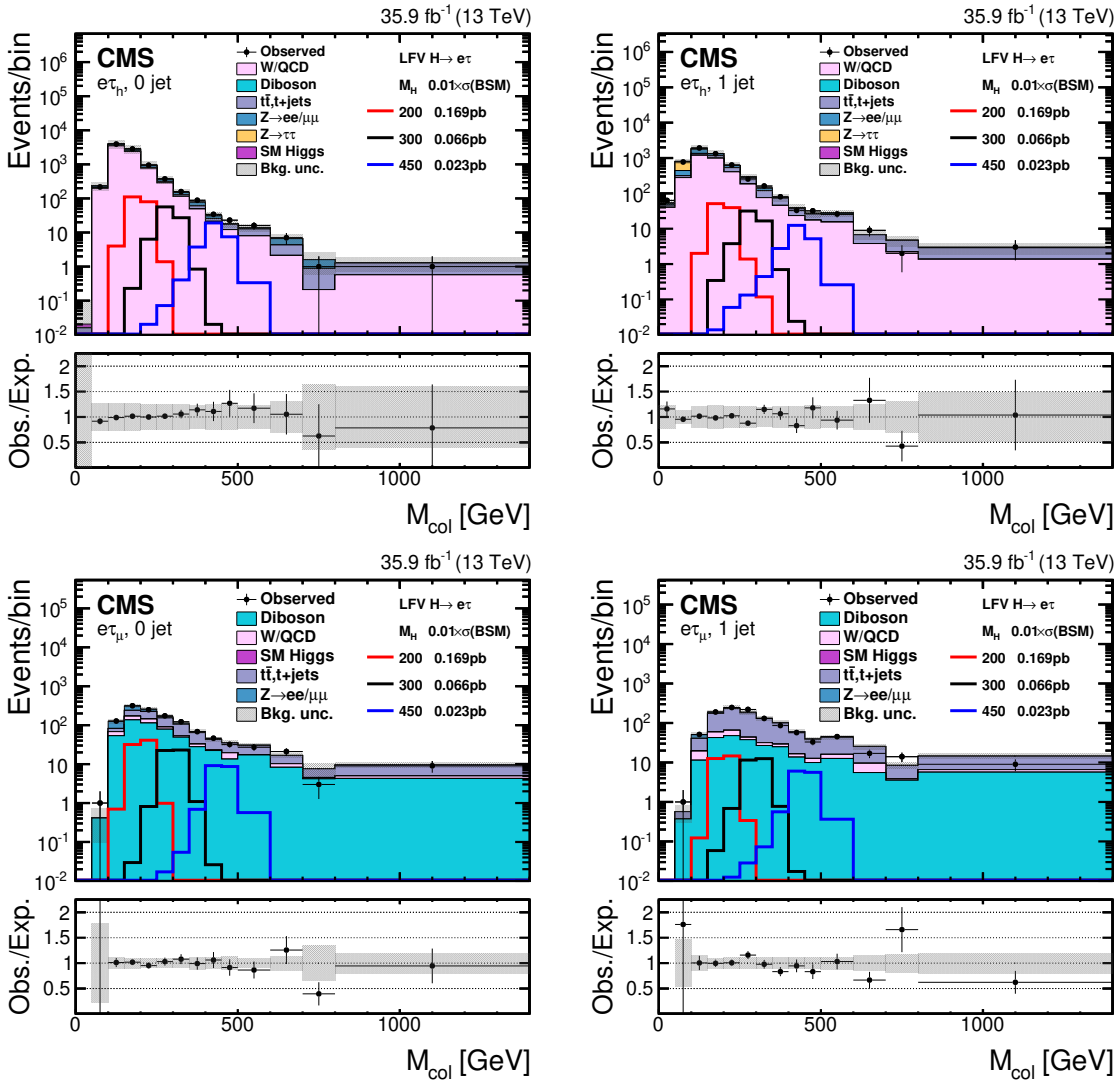

Figure 6. The M_{col} distribution in the signal region, for the $e\tau_h$ (upper) and $e\tau_\mu$ (lower) channels for the Higgs boson mass in the range 200–450 GeV for 0-jet (left) and 1-jet (right) categories. The uncertainty bands include both statistical and systematic uncertainties. The plotted values are number of events per bin using a variable bin size. The background is normalised to the best fit values from a binned likelihood fit, discussed in the text, to the background only hypothesis. For depicting the signals a branching fraction of 1% and BSM cross sections from ref. [79] are assumed.

analyses. Finally, we acknowledge the enduring support for the construction and operation of the LHC and the CMS detector provided by the following funding agencies: BMBWF and FWF (Austria); FNRS and FWO (Belgium); CNPq, CAPES, FAPERJ, FAPERGS, and FAPESP (Brazil); MES (Bulgaria); CERN; CAS, MoST, and NSFC (China); COLCIENCIAS (Colombia); MSES and CSF (Croatia); RPF (Cyprus); SENESCYT (Ecuador); MoER, ERC IUT, PUT and ERDF (Estonia); Academy of Finland, MEC, and HIP (Finland); CEA and CNRS/IN2P3 (France); BMBF, DFG, and HGF (Germany); GSRT (Greece); NKFIA (Hungary); DAE and DST (India); IPM (Iran); SFI (Ireland); INFN

JHEP03(2020)103

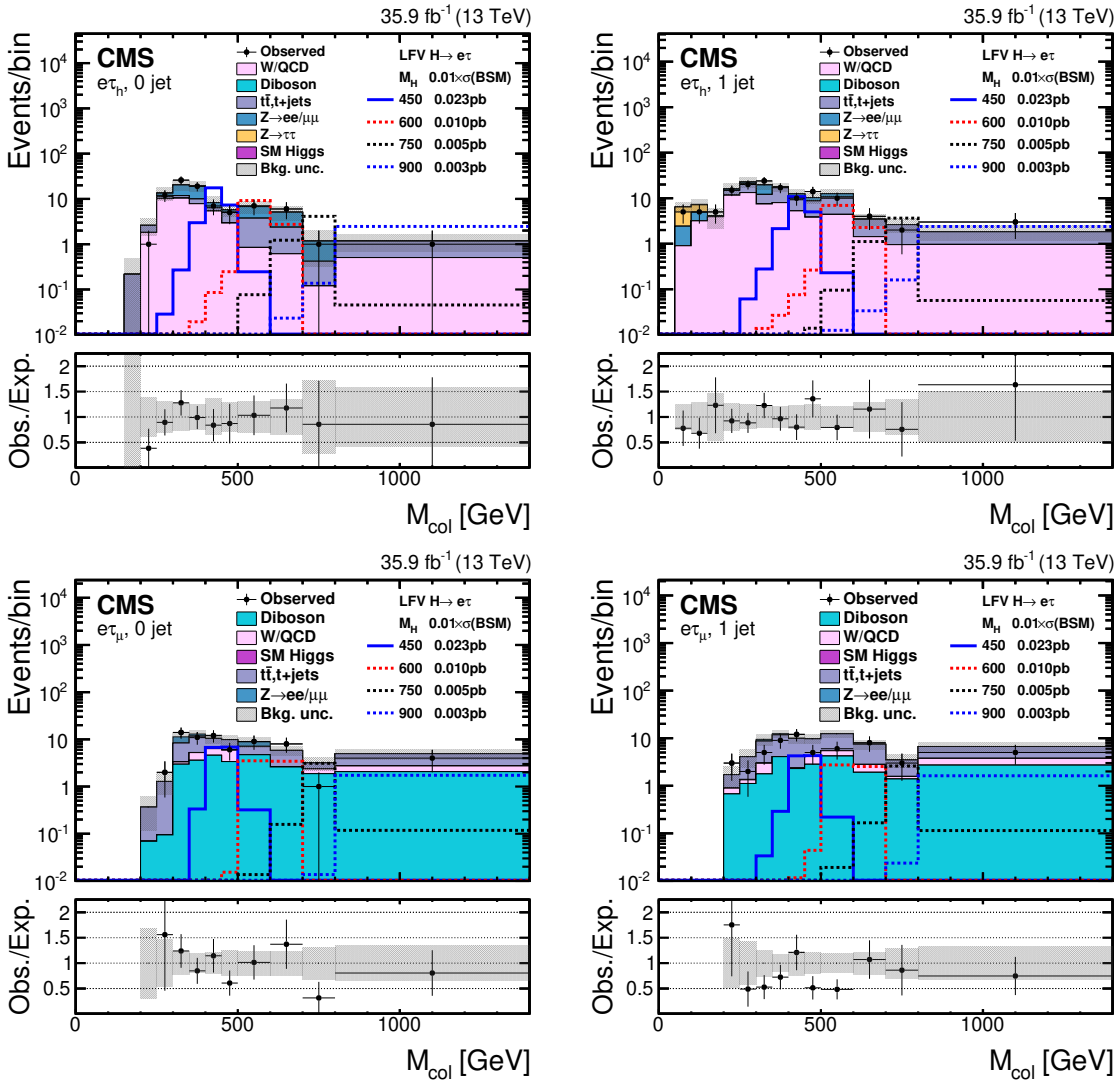

Figure 7. The M_{col} distribution in the signal region, for the $e\tau_h$ (upper) and $e\tau_\mu$ (lower) channels for the Higgs boson mass in the range 450–900 GeV for 0-jet (left) and 1-jet (right) categories. The uncertainty bands include both statistical and systematic uncertainties. The plotted values are number of events per bin using a variable bin size. The background is normalised to the best fit values from a binned likelihood fit, discussed in the text, to the background only hypothesis. For depicting the signals a branching fraction of 1% and BSM cross sections from ref. [79] are assumed.

(Italy); MSIP and NRF (Republic of Korea); MES (Latvia); LAS (Lithuania); MOE and UM (Malaysia); BUAP, CINVESTAV, CONACYT, LNS, SEP, and UASLP-FAI (Mexico); MOS (Montenegro); MBIE (New Zealand); PAEC (Pakistan); MSHE and NSC (Poland); FCT (Portugal); JINR (Dubna); MON, RosAtom, RAS, RFBR, and NRC KI (Russia); MESTD (Serbia); SEIDI, CPAN, PCTI, and FEDER (Spain); MOSTR (Sri Lanka); Swiss Funding Agencies (Switzerland); MST (Taipei); ThEPCenter, IPST, STAR, and NSTDA (Thailand); TUBITAK and TAEK (Turkey); NASU (Ukraine); STFC (United Kingdom); DOE and NSF (U.S.A.).

JHEP03(2020)103

Observed 95% CL upper limit on $\sigma(gg \to H)\mathcal{B}(H \to e\tau)$ (fb)									
	$e\tau_\mu$			$e\tau_h$			$e\tau$		
m_H (GeV)	0 jet	1 jet	comb	0 jet	1 jet	comb	0 jet	1 jet	comb
200	119.2	365.3	117.8	179.4	197.8	139.6	103.2	180.1	94.1
300	85.1	208.7	94.5	56.4	56.4	43.2	50.6	65.4	46.0
450	14.0	25.1	11.7	7.6	16.9	6.8	5.9	13.2	5.2
600	17.4	13.9	11.7	9.3	9.1	6.3	8.8	6.9	5.8
750	5.1	9.5	4.1	4.7	5.6	3.3	2.9	4.5	2.3
900	7.7	8.3	5.3	3.8	5.0	2.7	3.1	4.0	2.3

Median expected 95% CL upper limit on $\sigma(gg \to H)\mathcal{B}(H \to e\tau)$ (fb)									
	$e\tau_\mu$			$e\tau_h$			$e\tau$		
m_H (GeV)	0 jet	1 jet	comb	0 jet	1 jet	comb	0 jet	1 jet	comb
200	158.2	366.6	142.3	135.7	238.9	120.1	102.9	200.5	91.6
300	57.9	123.0	52.3	42.9	70.3	37.5	34.5	62.0	30.2
450	20.4	32.6	17.2	10.1	18.0	8.7	9.0	15.4	7.8
600	14.7	22.1	11.9	8.6	11.6	6.8	7.5	9.9	5.9
750	8.6	10.5	6.2	4.9	6.5	3.7	4.1	5.3	3.0
900	8.5	9.0	5.7	4.0	4.7	2.6	3.3	4.0	2.3

Table 6. The observed and median expected 95% CL upper limits on $\sigma(gg \to H)\mathcal{B}(H \to e\tau)$.

Individuals have received support from the Marie-Curie programme and the European Research Council and Horizon 2020 Grant, contract Nos. 675440, 752730, and 765710 (European Union); the Leventis Foundation; the A.P. Sloan Foundation; the Alexander von Humboldt Foundation; the Belgian Federal Science Policy Office; the Fonds pour la Formation à la Recherche dans l'Industrie et dans l'Agriculture (FRIA-Belgium); the Agentschap voor Innovatie door Wetenschap en Technologie (IWT-Belgium); the F.R.S.-FNRS and FWO (Belgium) under the "Excellence of Science — EOS" — be.h project n. 30820817; the Beijing Municipal Science & Technology Commission, No. Z181100004218003; the Ministry of Education, Youth and Sports (MEYS) of the Czech Republic; the Deutsche Forschungsgemeinschaft (DFG) under Germany's Excellence Strategy — EXC 2121 "Quantum Universe" — 390833306; the Lendület ("Momentum") Programme and the János Bolyai Research Scholarship of the Hungarian Academy of Sciences, the New National Excellence Program ÚNKP, the NKFIA research grants 123842, 123959, 124845, 124850, 125105, 128713, 128786, and 129058 (Hungary); the Council of Science and Industrial Research, India; the HOMING PLUS programme of the Foundation for Polish Science, cofinanced from European Union, Regional Development Fund, the Mobility Plus programme of the Ministry of Science and Higher Education, the National Science Center (Poland), contracts

JHEP03(2020)103

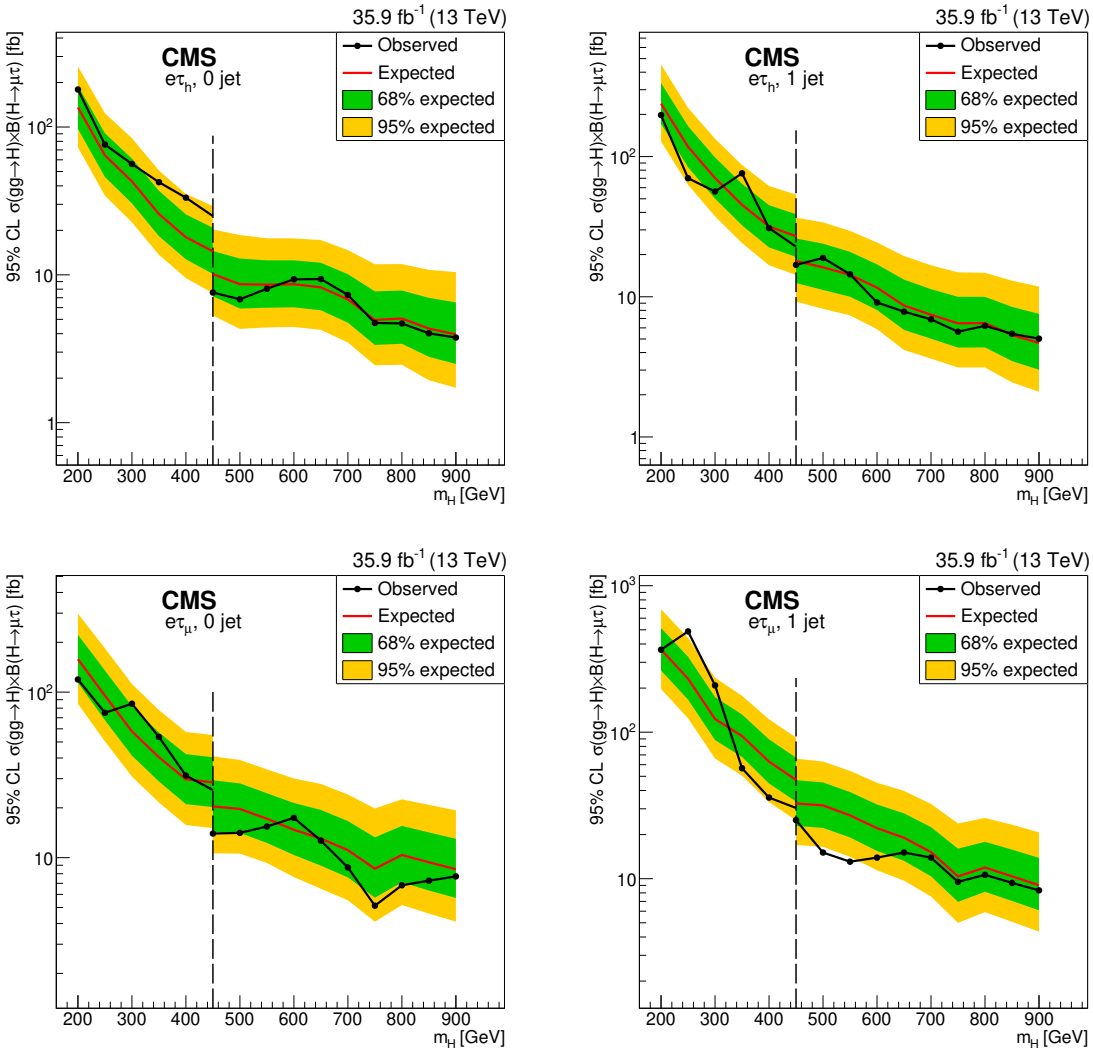

Figure 8. The observed and median expected 95% CL upper limits on $\sigma(\mathrm{gg} \to \mathrm{H})\mathcal{B}(\mathrm{H} \to \mathrm{e}\tau)$, for the $\mathrm{e}\tau_\mathrm{h}$ (upper) and $\mathrm{e}\tau_\mu$ (lower) channels, for 0-jet (left) and 1-jet (right) categories. The dashed line shows the transition between the two investigated mass ranges.

Harmonia 2014/14/M/ST2/00428, Opus 2014/13/B/ST2/02543, 2014/15/B/ST2/03998, and 2015/19/B/ST2/02861, Sonata-bis 2012/07/E/ST2/01406; the National Priorities Research Program by Qatar National Research Fund; the Ministry of Science and Education, grant no. 3.2989.2017 (Russia); the Programa Estatal de Fomento de la Investigación Científica y Técnica de Excelencia María de Maeztu, grant MDM-2015-0509 and the Programa Severo Ochoa del Principado de Asturias; the Thalis and Aristeia programmes cofinanced by EU-ESF and the Greek NSRF; the Rachadapisek Sompot Fund for Postdoctoral Fellowship, Chulalongkorn University and the Chulalongkorn Academic into Its 2nd Century Project Advancement Project (Thailand); the Nvidia Corporation; the Welch Foundation, contract C-1845; and the Weston Havens Foundation (U.S.A.).

JHEP03(2020)103

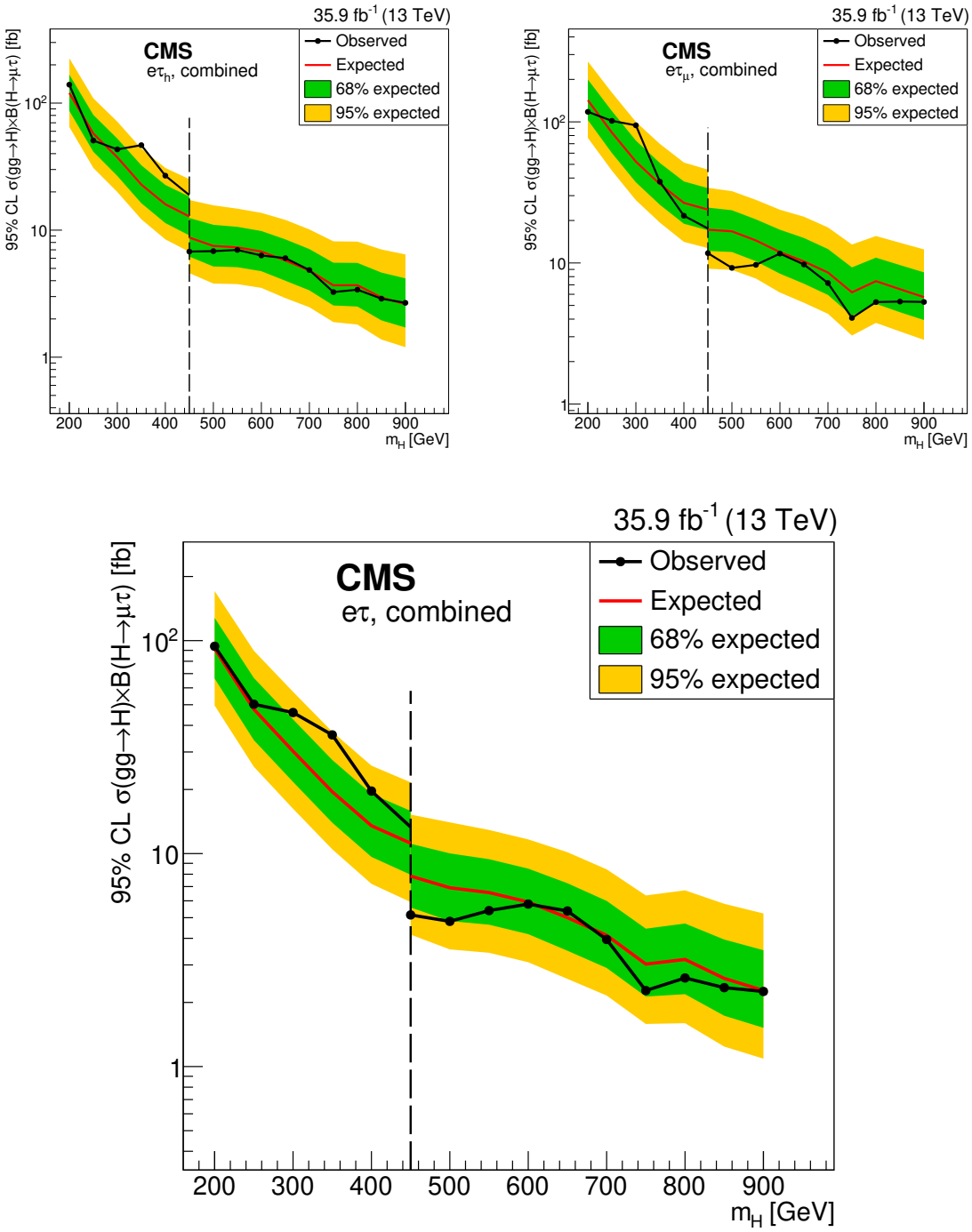

Figure 9. The combined observed and median expected 95% CL upper limits on $\sigma(gg \to H)\mathcal{B}(H \to e\tau)$, for $e\tau_h$ (upper left) and $e\tau_\mu$ (upper right) channels, and their combination $e\tau$ (lower). The dashed line shows the transition between the two investigated mass ranges.

JHEP03(2020)103

References

[1] ATLAS collaboration, *Observation of a new particle in the search for the Standard Model Higgs boson with the ATLAS detector at the LHC*, *Phys. Lett.* **B 716** (2012) 1 [arXiv:1207.7214] [INSPIRE].

[2] CMS collaboration, *Observation of a new boson at a mass of* 125 *GeV with the CMS experiment at the LHC*, *Phys. Lett.* **B 716** (2012) 30 [arXiv:1207.7235] [INSPIRE].

[3] CMS collaboration, *Observation of a new boson with mass near* 125 *GeV in pp collisions at* $\sqrt{s} = 7$ *and* 8 *TeV*, *JHEP* **06** (2013) 081 [arXiv:1303.4571] [INSPIRE].

[4] F. Englert and R. Brout, *Broken symmetry and the mass of gauge vector mesons*, *Phys. Rev. Lett.* **13** (1964) 321 [INSPIRE].

[5] P.W. Higgs, *Broken symmetries, massless particles and gauge fields*, *Phys. Lett.* **12** (1964) 132 [INSPIRE].

[6] P.W. Higgs, *Broken symmetries and the masses of gauge bosons*, *Phys. Rev. Lett.* **13** (1964) 508 [INSPIRE].

[7] G.S. Guralnik, C.R. Hagen and T.W.B. Kibble, *Global conservation laws and massless particles*, *Phys. Rev. Lett.* **13** (1964) 585 [INSPIRE].

[8] P.W. Higgs, *Spontaneous symmetry breakdown without massless bosons*, *Phys. Rev.* **145** (1966) 1156 [INSPIRE].

[9] T.W.B. Kibble, *Symmetry breaking in non-Abelian gauge theories*, *Phys. Rev.* **155** (1967) 1554 [INSPIRE].

[10] ATLAS and CMS collaborations, *Measurements of the Higgs boson production and decay rates and constraints on its couplings from a combined ATLAS and CMS analysis of the LHC pp collision data at* $\sqrt{s} = 7$ *and* 8 *TeV*, *JHEP* **08** (2016) 045 [arXiv:1606.02266] [INSPIRE].

[11] CMS collaboration, *Combined measurements of Higgs boson couplings in proton-proton collisions at* $\sqrt{s} = 13$ *TeV*, *Eur. Phys. J.* **C 79** (2019) 421 [arXiv:1809.10733] [INSPIRE].

[12] M. Buschmann, J. Kopp, J. Liu and X.-P. Wang, *New signatures of flavor violating Higgs couplings*, *JHEP* **06** (2016) 149 [arXiv:1601.02616] [INSPIRE].

[13] J.D. Bjorken and S. Weinberg, *A mechanism for nonconservation of muon number*, *Phys. Rev. Lett.* **38** (1977) 622 [INSPIRE].

[14] J.L. Diaz-Cruz and J.J. Toscano, *Lepton flavor violating decays of Higgs bosons beyond the Standard Model*, *Phys. Rev.* **D 62** (2000) 116005 [hep-ph/9910233] [INSPIRE].

[15] T. Han and D. Marfatia, $h \to \mu\tau$ *at hadron colliders*, *Phys. Rev. Lett.* **86** (2001) 1442 [hep-ph/0008141] [INSPIRE].

[16] E. Arganda, A.M. Curiel, M.J. Herrero and D. Temes, *Lepton flavor violating Higgs boson decays from massive seesaw neutrinos*, *Phys. Rev.* **D 71** (2005) 035011 [hep-ph/0407302] [INSPIRE].

JHEP03(2020)103

[17] A. Arhrib, Y. Cheng and O.C.W. Kong, *Comprehensive analysis on lepton flavor violating Higgs boson to $\mu^{\mp}\tau^{\pm}$ decay in supersymmetry without R parity*, *Phys. Rev.* **D 87** (2013) 015025 [arXiv:1210.8241] [INSPIRE].

[18] M. Arana-Catania, E. Arganda and M.J. Herrero, *Non-decoupling SUSY in LFV Higgs decays: a window to new physics at the LHC*, *JHEP* **09** (2013) 160 [*Erratum ibid.* **10** (2015) 192] [arXiv:1304.3371] [INSPIRE].

[19] E. Arganda, M.J. Herrero, R. Morales and A. Szynkman, *Analysis of the h, H, $A \to \tau\mu$ decays induced from SUSY loops within the mass insertion approximation*, *JHEP* **03** (2016) 055 [arXiv:1510.04685] [INSPIRE].

[20] E. Arganda, M.J. Herrero, X. Marcano and C. Weiland, *Enhancement of the lepton flavor violating Higgs boson decay rates from SUSY loops in the inverse seesaw model*, *Phys. Rev.* **D 93** (2016) 055010 [arXiv:1508.04623] [INSPIRE].

[21] K. Agashe and R. Contino, *Composite Higgs-mediated FCNC*, *Phys. Rev.* **D 80** (2009) 075016 [arXiv:0906.1542] [INSPIRE].

[22] A. Azatov, M. Toharia and L. Zhu, *Higgs mediated FCNC's in warped extra dimensions*, *Phys. Rev.* **D 80** (2009) 035016 [arXiv:0906.1990] [INSPIRE].

[23] H. Ishimori, T. Kobayashi, H. Ohki, Y. Shimizu, H. Okada and M. Tanimoto, *Non-Abelian discrete symmetries in particle physics*, *Prog. Theor. Phys. Suppl.* **183** (2010) 1 [arXiv:1003.3552] [INSPIRE].

[24] G. Perez and L. Randall, *Natural neutrino masses and mixings from warped geometry*, *JHEP* **01** (2009) 077 [arXiv:0805.4652] [INSPIRE].

[25] S. Casagrande, F. Goertz, U. Haisch, M. Neubert and T. Pfoh, *Flavor physics in the Randall-Sundrum model: I. Theoretical setup and electroweak precision tests*, *JHEP* **10** (2008) 094 [arXiv:0807.4937] [INSPIRE].

[26] A.J. Buras, B. Duling and S. Gori, *The impact of Kaluza-Klein fermions on Standard Model fermion couplings in a RS model with custodial protection*, *JHEP* **09** (2009) 076 [arXiv:0905.2318] [INSPIRE].

[27] M. Blanke, A.J. Buras, B. Duling, S. Gori and A. Weiler, *$\Delta F = 2$ observables and fine-tuning in a warped extra dimension with custodial protection*, *JHEP* **03** (2009) 001 [arXiv:0809.1073] [INSPIRE].

[28] G.F. Giudice and O. Lebedev, *Higgs-dependent Yukawa couplings*, *Phys. Lett.* **B 665** (2008) 79 [arXiv:0804.1753] [INSPIRE].

[29] J.A. Aguilar-Saavedra, *A minimal set of top-Higgs anomalous couplings*, *Nucl. Phys.* **B 821** (2009) 215 [arXiv:0904.2387] [INSPIRE].

[30] M.E. Albrecht, M. Blanke, A.J. Buras, B. Duling and K. Gemmler, *Electroweak and flavour structure of a warped extra dimension with custodial protection*, *JHEP* **09** (2009) 064 [arXiv:0903.2415] [INSPIRE].

[31] A. Goudelis, O. Lebedev and J.-H. Park, *Higgs-induced lepton flavor violation*, *Phys. Lett.* **B 707** (2012) 369 [arXiv:1111.1715] [INSPIRE].

[32] D. McKeen, M. Pospelov and A. Ritz, *Modified Higgs branching ratios versus CP and lepton flavor violation*, *Phys. Rev.* **D 86** (2012) 113004 [arXiv:1208.4597] [INSPIRE].

JHEP03(2020)103

[33] A. Pilaftsis, *Lepton flavor nonconservation in H^0 decays*, *Phys. Lett.* **B 285** (1992) 68 [INSPIRE].

[34] J.G. Körner, A. Pilaftsis and K. Schilcher, *Leptonic CP asymmetries in flavor changing H^0 decays*, *Phys. Rev.* **D 47** (1993) 1080 [hep-ph/9301289] [INSPIRE].

[35] E. Arganda, M.J. Herrero, X. Marcano and C. Weiland, *Imprints of massive inverse seesaw model neutrinos in lepton flavor violating Higgs boson decays*, *Phys. Rev.* **D 91** (2015) 015001 [arXiv:1405.4300] [INSPIRE].

[36] M. Sher and K. Thrasher, *Flavor changing leptonic decays of heavy Higgs bosons*, *Phys. Rev.* **D 93** (2016) 055021 [arXiv:1601.03973] [INSPIRE].

[37] E. Arganda, X. Marcano, N.I. Mileo, R.A. Morales and A. Szynkman, *Model-independent search strategy for the lepton-flavor-violating heavy Higgs boson decay to $\tau\mu$ at the LHC*, *Eur. Phys. J.* **C 79** (2019) 738 [arXiv:1906.08282] [INSPIRE].

[38] CMS collaboration, *Search for lepton flavour violating decays of the Higgs boson to $\mu\tau$ and $e\tau$ in proton-proton collisions at $\sqrt{s} = 13$ TeV*, *JHEP* **06** (2018) 001 [arXiv:1712.07173] [INSPIRE].

[39] CMS collaboration, *Search for lepton-flavour-violating decays of the Higgs boson*, *Phys. Lett.* **B 749** (2015) 337 [arXiv:1502.07400] [INSPIRE].

[40] CMS collaboration, *Search for lepton flavour violating decays of the Higgs boson to $e\tau$ and $e\mu$ in proton-proton collisions at $\sqrt{s} = 8$ TeV*, *Phys. Lett.* **B 763** (2016) 472 [arXiv:1607.03561] [INSPIRE].

[41] ATLAS collaboration, *Search for lepton-flavour-violating decays of the Higgs and Z bosons with the ATLAS detector*, *Eur. Phys. J.* **C 77** (2017) 70 [arXiv:1604.07730] [INSPIRE].

[42] ATLAS collaboration, *Search for lepton-flavour-violating $H \to \mu\tau$ decays of the Higgs boson with the ATLAS detector*, *JHEP* **11** (2015) 211 [arXiv:1508.03372] [INSPIRE].

[43] CMS collaboration, *Evidence for the direct decay of the 125 GeV Higgs boson to fermions*, *Nature Phys.* **10** (2014) 557 [arXiv:1401.6527] [INSPIRE].

[44] CMS collaboration, *Evidence for the 125 GeV Higgs boson decaying to a pair of τ leptons*, *JHEP* **05** (2014) 104 [arXiv:1401.5041] [INSPIRE].

[45] CMS collaboration, *Observation of the Higgs boson decay to a pair of τ leptons with the CMS detector*, *Phys. Lett.* **B 779** (2018) 283 [arXiv:1708.00373] [INSPIRE].

[46] CMS collaboration, *Search for neutral MSSM Higgs bosons decaying to a pair of tau leptons in pp collisions*, *JHEP* **10** (2014) 160 [arXiv:1408.3316] [INSPIRE].

[47] ATLAS collaboration, *Evidence for the Higgs-boson Yukawa coupling to tau leptons with the ATLAS detector*, *JHEP* **04** (2015) 117 [arXiv:1501.04943] [INSPIRE].

[48] CMS collaboration, *The CMS experiment at the CERN LHC*, 2008 *JINST* **3** S08004 [INSPIRE].

[49] CMS collaboration, *The CMS trigger system*, 2017 *JINST* **12** P01020 [arXiv:1609.02366] [INSPIRE].

[50] CMS collaboration, *CMS luminosity measurements for the 2016 data taking period*, CMS-PAS-LUM-17-001, CERN, Geneva, Switzerland (2017).

[51] P. Nason, *A new method for combining NLO QCD with shower Monte Carlo algorithms*, *JHEP* **11** (2004) 040 [hep-ph/0409146] [INSPIRE].

JHEP03(2020)103

[52] S. Frixione, P. Nason and C. Oleari, *Matching NLO QCD computations with parton shower simulations: the POWHEG method*, *JHEP* **11** (2007) 070 [arXiv:0709.2092] [INSPIRE].

[53] S. Alioli, P. Nason, C. Oleari and E. Re, *A general framework for implementing NLO calculations in shower Monte Carlo programs: the POWHEG BOX*, *JHEP* **06** (2010) 043 [arXiv:1002.2581] [INSPIRE].

[54] S. Alioli, K. Hamilton, P. Nason, C. Oleari and E. Re, *Jet pair production in POWHEG*, *JHEP* **04** (2011) 081 [arXiv:1012.3380] [INSPIRE].

[55] S. Alioli, P. Nason, C. Oleari and E. Re, *NLO Higgs boson production via gluon fusion matched with shower in POWHEG*, *JHEP* **04** (2009) 002 [arXiv:0812.0578] [INSPIRE].

[56] E. Bagnaschi, G. Degrassi, P. Slavich and A. Vicini, *Higgs production via gluon fusion in the POWHEG approach in the SM and in the MSSM*, *JHEP* **02** (2012) 088 [arXiv:1111.2854] [INSPIRE].

[57] H.M. Georgi, S.L. Glashow, M.E. Machacek and D.V. Nanopoulos, *Higgs bosons from two gluon annihilation in proton proton collisions*, *Phys. Rev. Lett.* **40** (1978) 692 [INSPIRE].

[58] J. Alwall et al., *The automated computation of tree-level and next-to-leading order differential cross sections and their matching to parton shower simulations*, *JHEP* **07** (2014) 079 [arXiv:1405.0301] [INSPIRE].

[59] J. Alwall et al., *Comparative study of various algorithms for the merging of parton showers and matrix elements in hadronic collisions*, *Eur. Phys. J.* **C 53** (2008) 473 [arXiv:0706.2569] [INSPIRE].

[60] R. Frederix and S. Frixione, *Merging meets matching in MC@NLO*, *JHEP* **12** (2012) 061 [arXiv:1209.6215] [INSPIRE].

[61] T. Sjöstrand et al., *An introduction to PYTHIA* 8.2, *Comput. Phys. Commun.* **191** (2015) 159 [arXiv:1410.3012] [INSPIRE].

[62] CMS collaboration, *Event generator tunes obtained from underlying event and multiparton scattering measurements*, *Eur. Phys. J.* **C 76** (2016) 155 [arXiv:1512.00815] [INSPIRE].

[63] NNPDF collaboration, *Unbiased global determination of parton distributions and their uncertainties at NNLO and at LO*, *Nucl. Phys.* **B 855** (2012) 153 [arXiv:1107.2652] [INSPIRE].

[64] GEANT4 collaboration, *GEANT4: a simulation toolkit*, *Nucl. Instrum. Meth.* **A 506** (2003) 250 [INSPIRE].

[65] CMS collaboration, *Particle-flow reconstruction and global event description with the CMS detector*, 2017 *JINST* **12** P10003 [arXiv:1706.04965] [INSPIRE].

[66] M. Cacciari, G.P. Salam and G. Soyez, *The anti-k_t jet clustering algorithm*, *JHEP* **04** (2008) 063 [arXiv:0802.1189] [INSPIRE].

[67] M. Cacciari, G.P. Salam and G. Soyez, *FastJet user manual*, *Eur. Phys. J.* **C 72** (2012) 1896 [arXiv:1111.6097] [INSPIRE].

[68] CMS collaboration, *Performance of the CMS muon detector and muon reconstruction with proton-proton collisions at $\sqrt{s} = 13$ TeV*, 2018 *JINST* **13** P06015 [arXiv:1804.04528] [INSPIRE].

[69] CMS collaboration, *Performance of electron reconstruction and selection with the CMS detector in proton-proton collisions at $\sqrt{s} = 8$ TeV*, 2015 *JINST* **10** P06005 [arXiv:1502.02701] [INSPIRE].

JHEP03(2020)103

[70] M. Cacciari and G.P. Salam, *Dispelling the N^3 myth for the k_t jet-finder*, *Phys. Lett.* **B 641** (2006) 57 [hep-ph/0512210] [INSPIRE].

[71] CMS collaboration, *Jet energy scale and resolution in the CMS experiment in pp collisions at 8 TeV*, 2017 *JINST* **12** P02014 [arXiv:1607.03663] [INSPIRE].

[72] CMS collaboration, *Reconstruction and identification of τ lepton decays to hadrons and ν_τ at CMS*, 2016 *JINST* **11** P01019 [arXiv:1510.07488] [INSPIRE].

[73] CMS collaboration, *Performance of reconstruction and identification of τ leptons decaying to hadrons and ν_τ in pp collisions at $\sqrt{s} = 13$ TeV*, 2018 *JINST* **13** P10005 [arXiv:1809.02816] [INSPIRE].

[74] M. Cacciari, G.P. Salam and G. Soyez, *The catchment area of jets*, *JHEP* **04** (2008) 005 [arXiv:0802.1188] [INSPIRE].

[75] M. Cacciari and G.P. Salam, *Pileup subtraction using jet areas*, *Phys. Lett.* **B 659** (2008) 119 [arXiv:0707.1378] [INSPIRE].

[76] CMS collaboration, *Identification of heavy-flavour jets with the CMS detector in pp collisions at 13 TeV*, 2018 *JINST* **13** P05011 [arXiv:1712.07158] [INSPIRE].

[77] CMS collaboration, *Performance of missing transverse momentum reconstruction in proton-proton collisions at $\sqrt{s} = 13$ TeV using the CMS detector*, 2019 *JINST* **14** P07004 [arXiv:1903.06078] [INSPIRE].

[78] R.K. Ellis, I. Hinchliffe, M. Soldate and J.J. van der Bij, *Higgs decay to $\tau^+\tau^-$: a possible signature of intermediate mass Higgs bosons at the SSC*, *Nucl. Phys.* **B 297** (1988) 221 [INSPIRE].

[79] LHC Higgs Cross Section Working Group collaboration, *Handbook of LHC Higgs cross sections: 4. Deciphering the nature of the Higgs sector*, CYRM-2017-002, CERN, Geneva, Switzerland (2016) [arXiv:1610.07922] [INSPIRE].

[80] R.J. Barlow and C. Beeston, *Fitting using finite Monte Carlo samples*, *Comput. Phys. Commun.* **77** (1993) 219 [INSPIRE].

[81] CMS collaboration, *Measurement of the inelastic proton-proton cross section at $\sqrt{s} = 13$ TeV*, *JHEP* **07** (2018) 161 [arXiv:1802.02613] [INSPIRE].

[82] J.S. Conway, *Incorporating nuisance parameters in likelihoods for multisource spectra*, in *Proceedings, PHYSTAT* 2011 *Workshop on Statistical Issues Related to Discovery Claims in Search Experiments and Unfolding*, CERN, Geneva, Switzerland 17–20 January 2011, CERN-2011-006, CERN, Geneva, Switzerland (2011), pg. 115 [arXiv:1103.0354] [INSPIRE].

[83] ATLAS, CMS collaborations and the LHC Higgs Combination Group, *Procedure for the LHC Higgs boson search combination in Summer* 2011, ATL-PHYS-PUB-2011-11, CERN, Geneva, Switzerland (2011) [CMS-NOTE-2011-005].

[84] T. Junk, *Confidence level computation for combining searches with small statistics*, *Nucl. Instrum. Meth.* **A 434** (1999) 435 [hep-ex/9902006] [INSPIRE].

[85] A.L. Read, *Presentation of search results: the CL_s technique*, *J. Phys.* **G 28** (2002) 2693 [INSPIRE].

[86] G. Cowan, K. Cranmer, E. Gross and O. Vitells, *Asymptotic formulae for likelihood-based tests of new physics*, *Eur. Phys. J.* **C 71** (2011) 1554 [*Erratum ibid.* **C 73** (2013) 2501] [arXiv:1007.1727] [INSPIRE].

JHEP03(2020)103

The CMS collaboration

Yerevan Physics Institute, Yerevan, Armenia

A.M. Sirunyan[†], A. Tumasyan

Institut für Hochenergiephysik, Wien, Austria

W. Adam, F. Ambrogi, T. Bergauer, J. Brandstetter, M. Dragicevic, J. Erö, A. Escalante Del Valle, M. Flechl, R. Frühwirth[1], M. Jeitler[1], N. Krammer, I. Krätschmer, D. Liko, T. Madlener, I. Mikulec, N. Rad, J. Schieck[1], R. Schöfbeck, M. Spanring, D. Spitzbart, W. Waltenberger, C.-E. Wulz[1], M. Zarucki

Institute for Nuclear Problems, Minsk, Belarus

V. Drugakov, V. Mossolov, J. Suarez Gonzalez

Universiteit Antwerpen, Antwerpen, Belgium

M.R. Darwish, E.A. De Wolf, D. Di Croce, X. Janssen, J. Lauwers, A. Lelek, M. Pieters, H. Rejeb Sfar, H. Van Haevermaet, P. Van Mechelen, S. Van Putte, N. Van Remortel

Vrije Universiteit Brussel, Brussel, Belgium

F. Blekman, E.S. Bols, S.S. Chhibra, J. D'Hondt, J. De Clercq, D. Lontkovskyi, S. Lowette, I. Marchesini, S. Moortgat, L. Moreels, Q. Python, K. Skovpen, S. Tavernier, W. Van Doninck, P. Van Mulders, I. Van Parijs

Université Libre de Bruxelles, Bruxelles, Belgium

D. Beghin, B. Bilin, H. Brun, B. Clerbaux, G. De Lentdecker, H. Delannoy, B. Dorney, L. Favart, A. Grebenyuk, A.K. Kalsi, J. Luetic, A. Popov, N. Postiau, E. Starling, L. Thomas, C. Vander Velde, P. Vanlaer, D. Vannerom

Ghent University, Ghent, Belgium

T. Cornelis, D. Dobur, I. Khvastunov[2], M. Niedziela, C. Roskas, D. Trocino, M. Tytgat, W. Verbeke, B. Vermassen, M. Vit, N. Zaganidis

Université Catholique de Louvain, Louvain-la-Neuve, Belgium

O. Bondu, G. Bruno, C. Caputo, P. David, C. Delaere, M. Delcourt, A. Giammanco, V. Lemaitre, A. Magitteri, J. Prisciandaro, A. Saggio, M. Vidal Marono, P. Vischia, J. Zobec

Centro Brasileiro de Pesquisas Fisicas, Rio de Janeiro, Brazil

F.L. Alves, G.A. Alves, G. Correia Silva, C. Hensel, A. Moraes, P. Rebello Teles

Universidade do Estado do Rio de Janeiro, Rio de Janeiro, Brazil

E. Belchior Batista Das Chagas, W. Carvalho, J. Chinellato[3], E. Coelho, E.M. Da Costa, G.G. Da Silveira[4], D. De Jesus Damiao, C. De Oliveira Martins, S. Fonseca De Souza, L.M. Huertas Guativa, H. Malbouisson, J. Martins[5], D. Matos Figueiredo, M. Medina Jaime[6], M. Melo De Almeida, C. Mora Herrera, L. Mundim, H. Nogima, W.L. Prado Da Silva, L.J. Sanchez Rosas, A. Santoro, A. Sznajder, M. Thiel, E.J. Tonelli Manganote[3], F. Torres Da Silva De Araujo, A. Vilela Pereira

JHEP03(2020)103

Universidade Estadual Paulista [a], Universidade Federal do ABC [b], São Paulo, Brazil

S. Ahuja[a], C.A. Bernardes[a], L. Calligaris[a], T.R. Fernandez Perez Tomei[a], E.M. Gregores[b], D.S. Lemos, P.G. Mercadante[b], S.F. Novaes[a], SandraS. Padula[a]

Institute for Nuclear Research and Nuclear Energy, Bulgarian Academy of Sciences, Sofia, Bulgaria

A. Aleksandrov, G. Antchev, R. Hadjiiska, P. Iaydjiev, A. Marinov, M. Misheva, M. Rodozov, M. Shopova, G. Sultanov

University of Sofia, Sofia, Bulgaria

M. Bonchev, A. Dimitrov, T. Ivanov, L. Litov, B. Pavlov, P. Petkov

Beihang University, Beijing, China

W. Fang[7], X. Gao[7], L. Yuan

Department of Physics, Tsinghua University, Beijing, China

Z. Hu, Y. Wang

Institute of High Energy Physics, Beijing, China

M. Ahmad, G.M. Chen, H.S. Chen, M. Chen, C.H. Jiang, D. Leggat, H. Liao, Z. Liu, S.M. Shaheen[8], A. Spiezia, J. Tao, E. Yazgan, H. Zhang, S. Zhang[8], J. Zhao

State Key Laboratory of Nuclear Physics and Technology, Peking University, Beijing, China

A. Agapitos, Y. Ban, G. Chen, A. Levin, J. Li, L. Li, Q. Li, Y. Mao, S.J. Qian, D. Wang, Q. Wang

Universidad de Los Andes, Bogota, Colombia

C. Avila, A. Cabrera, L.F. Chaparro Sierra, C. Florez, C.F. González Hernández, M.A. Segura Delgado

Universidad de Antioquia, Medellin, Colombia

J. Mejia Guisao, J.D. Ruiz Alvarez, C.A. Salazar González, N. Vanegas Arbelaez

University of Split, Faculty of Electrical Engineering, Mechanical Engineering and Naval Architecture, Split, Croatia

D. Giljanović, N. Godinovic, D. Lelas, I. Puljak, T. Sculac

University of Split, Faculty of Science, Split, Croatia

Z. Antunovic, M. Kovac

Institute Rudjer Boskovic, Zagreb, Croatia

V. Brigljevic, S. Ceci, D. Ferencek, K. Kadija, B. Mesic, M. Roguljic, A. Starodumov[9], T. Susa

University of Cyprus, Nicosia, Cyprus

M.W. Ather, A. Attikis, E. Erodotou, A. Ioannou, M. Kolosova, S. Konstantinou, G. Mavromanolakis, J. Mousa, C. Nicolaou, F. Ptochos, P.A. Razis, H. Rykaczewski, D. Tsiakkouri

JHEP03(2020)103

Charles University, Prague, Czech Republic
M. Finger[10], M. Finger Jr.[10], A. Kveton, J. Tomsa

Escuela Politecnica Nacional, Quito, Ecuador
E. Ayala

Universidad San Francisco de Quito, Quito, Ecuador
E. Carrera Jarrin

Academy of Scientific Research and Technology of the Arab Republic of Egypt, Egyptian Network of High Energy Physics, Cairo, Egypt
H. Abdalla[11], E. Salama[12,13]

National Institute of Chemical Physics and Biophysics, Tallinn, Estonia
S. Bhowmik, A. Carvalho Antunes De Oliveira, R.K. Dewanjee, K. Ehataht, M. Kadastik, M. Raidal, C. Veelken

Department of Physics, University of Helsinki, Helsinki, Finland
P. Eerola, L. Forthomme, H. Kirschenmann, K. Osterberg, M. Voutilainen

Helsinki Institute of Physics, Helsinki, Finland
F. Garcia, J. Havukainen, J.K. Heikkilä, T. Järvinen, V. Karimäki, R. Kinnunen, T. Lampén, K. Lassila-Perini, S. Laurila, S. Lehti, T. Lindén, P. Luukka, T. Mäenpää, H. Siikonen, E. Tuominen, J. Tuominiemi

Lappeenranta University of Technology, Lappeenranta, Finland
T. Tuuva

IRFU, CEA, Université Paris-Saclay, Gif-sur-Yvette, France
M. Besancon, F. Couderc, M. Dejardin, D. Denegri, B. Fabbro, J.L. Faure, F. Ferri, S. Ganjour, A. Givernaud, P. Gras, G. Hamel de Monchenault, P. Jarry, C. Leloup, E. Locci, J. Malcles, J. Rander, A. Rosowsky, M.Ö. Sahin, A. Savoy-Navarro[14], M. Titov

Laboratoire Leprince-Ringuet, CNRS/IN2P3, Ecole Polytechnique, Institut Polytechnique de Paris
C. Amendola, F. Beaudette, P. Busson, C. Charlot, B. Diab, G. Falmagne, R. Granier de Cassagnac, I. Kucher, A. Lobanov, C. Martin Perez, M. Nguyen, C. Ochando, P. Paganini, J. Rembser, R. Salerno, J.B. Sauvan, Y. Sirois, A. Zabi, A. Zghiche

Université de Strasbourg, CNRS, IPHC UMR 7178, Strasbourg, France
J.-L. Agram[15], J. Andrea, D. Bloch, G. Bourgatte, J.-M. Brom, E.C. Chabert, C. Collard, E. Conte[15], J.-C. Fontaine[15], D. Gelé, U. Goerlach, M. Jansová, A.-C. Le Bihan, N. Tonon, P. Van Hove

Centre de Calcul de l'Institut National de Physique Nucleaire et de Physique des Particules, CNRS/IN2P3, Villeurbanne, France
S. Gadrat

JHEP03(2020)103

Université de Lyon, Université Claude Bernard Lyon 1, CNRS-IN2P3, Institut de Physique Nucléaire de Lyon, Villeurbanne, France
S. Beauceron, C. Bernet, G. Boudoul, C. Camen, N. Chanon, R. Chierici, D. Contardo, P. Depasse, H. El Mamouni, J. Fay, S. Gascon, M. Gouzevitch, B. Ille, Sa. Jain, F. Lagarde, I.B. Laktineh, H. Lattaud, M. Lethuillier, L. Mirabito, S. Perries, V. Sordini, G. Touquet, M. Vander Donckt, S. Viret

Georgian Technical University, Tbilisi, Georgia
A. Khvedelidze[10]

Tbilisi State University, Tbilisi, Georgia
Z. Tsamalaidze[10]

RWTH Aachen University, I. Physikalisches Institut, Aachen, Germany
C. Autermann, L. Feld, M.K. Kiesel, K. Klein, M. Lipinski, D. Meuser, A. Pauls, M. Preuten, M.P. Rauch, C. Schomakers, J. Schulz, M. Teroerde, B. Wittmer

RWTH Aachen University, III. Physikalisches Institut A, Aachen, Germany
A. Albert, M. Erdmann, S. Erdweg, T. Esch, B. Fischer, R. Fischer, S. Ghosh, T. Hebbeker, K. Hoepfner, H. Keller, L. Mastrolorenzo, M. Merschmeyer, A. Meyer, P. Millet, G. Mocellin, S. Mondal, S. Mukherjee, D. Noll, A. Novak, T. Pook, A. Pozdnyakov, T. Quast, M. Radziej, Y. Rath, H. Reithler, M. Rieger, J. Roemer, A. Schmidt, S.C. Schuler, A. Sharma, S. Thüer, S. Wiedenbeck

RWTH Aachen University, III. Physikalisches Institut B, Aachen, Germany
G. Flügge, W. Haj Ahmad[16], O. Hlushchenko, T. Kress, T. Müller, A. Nehrkorn, A. Nowack, C. Pistone, O. Pooth, D. Roy, H. Sert, A. Stahl[17]

Deutsches Elektronen-Synchrotron, Hamburg, Germany
M. Aldaya Martin, P. Asmuss, I. Babounikau, H. Bakhshiansohi, K. Beernaert, O. Behnke, U. Behrens, A. Bermúdez Martínez, D. Bertsche, A.A. Bin Anuar, K. Borras[18], V. Botta, A. Campbell, A. Cardini, P. Connor, S. Consuegra Rodríguez, C. Contreras-Campana, V. Danilov, A. De Wit, M.M. Defranchis, C. Diez Pardos, D. Domínguez Damiani, G. Eckerlin, D. Eckstein, T. Eichhorn, A. Elwood, E. Eren, E. Gallo[19], A. Geiser, J.M. Grados Luyando, A. Grohsjean, M. Guthoff, M. Haranko, A. Harb, A. Jafari, N.Z. Jomhari, H. Jung, A. Kasem[18], M. Kasemann, H. Kaveh, J. Keaveney, C. Kleinwort, J. Knolle, D. Krücker, W. Lange, T. Lenz, J. Leonard, J. Lidrych, K. Lipka, W. Lohmann[20], R. Mankel, I.-A. Melzer-Pellmann, A.B. Meyer, M. Meyer, M. Missiroli, G. Mittag, J. Mnich, A. Mussgiller, V. Myronenko, D. Pérez Adán, S.K. Pflitsch, D. Pitzl, A. Raspereza, A. Saibel, M. Savitskyi, V. Scheurer, P. Schütze, C. Schwanenberger, R. Shevchenko, A. Singh, H. Tholen, O. Turkot, A. Vagnerini, M. Van De Klundert, G.P. Van Onsem, R. Walsh, Y. Wen, K. Wichmann, C. Wissing, O. Zenaiev, R. Zlebcik

University of Hamburg, Hamburg, Germany
R. Aggleton, S. Bein, L. Benato, A. Benecke, V. Blobel, T. Dreyer, A. Ebrahimi, A. Fröhlich, C. Garbers, E. Garutti, D. Gonzalez, P. Gunnellini, J. Haller, A. Hinzmann, A. Karavdina, G. Kasieczka, R. Klanner, R. Kogler, N. Kovalchuk, S. Kurz, V. Kutzner,

JHEP03(2020)103

J. Lange, T. Lange, A. Malara, D. Marconi, J. Multhaup, C.E.N. Niemeyer, D. Nowatschin, A. Perieanu, A. Reimers, O. Rieger, C. Scharf, P. Schleper, S. Schumann, J. Schwandt, J. Sonneveld, H. Stadie, G. Steinbrück, F.M. Stober, M. Stöver, B. Vormwald, I. Zoi

Karlsruher Institut fuer Technologie, Karlsruhe, Germany
M. Akbiyik, C. Barth, M. Baselga, S. Baur, T. Berger, E. Butz, R. Caspart, T. Chwalek, W. De Boer, A. Dierlamm, K. El Morabit, N. Faltermann, M. Giffels, P. Goldenzweig, A. Gottmann, M.A. Harrendorf, F. Hartmann[17], U. Husemann, S. Kudella, S. Mitra, M.U. Mozer, Th. Müller, M. Musich, A. Nürnberg, G. Quast, K. Rabbertz, M. Schröder, I. Shvetsov, H.J. Simonis, R. Ulrich, M. Weber, C. Wöhrmann, R. Wolf

Institute of Nuclear and Particle Physics (INPP), NCSR Demokritos, Aghia Paraskevi, Greece
G. Anagnostou, P. Asenov, G. Daskalakis, T. Geralis, A. Kyriakis, D. Loukas, G. Paspalaki

National and Kapodistrian University of Athens, Athens, Greece
M. Diamantopoulou, G. Karathanasis, P. Kontaxakis, A. Panagiotou, I. Papavergou, N. Saoulidou, A. Stakia, K. Theofilatos, K. Vellidis

National Technical University of Athens, Athens, Greece
G. Bakas, K. Kousouris, I. Papakrivopoulos, G. Tsipolitis

University of Ioánnina, Ioánnina, Greece
I. Evangelou, C. Foudas, P. Gianneios, P. Katsoulis, P. Kokkas, S. Mallios, K. Manitara, N. Manthos, I. Papadopoulos, J. Strologas, F.A. Triantis, D. Tsitsonis

MTA-ELTE Lendület CMS Particle and Nuclear Physics Group, Eötvös Loránd University, Budapest, Hungary
M. Bartók[21], M. Csanad, P. Major, K. Mandal, A. Mehta, M.I. Nagy, G. Pasztor, O. Surányi, G.I. Veres

Wigner Research Centre for Physics, Budapest, Hungary
G. Bencze, C. Hajdu, D. Horvath[22], F. Sikler, T.Á. Vámi, V. Veszpremi, G. Vesztergombi[†]

Institute of Nuclear Research ATOMKI, Debrecen, Hungary
N. Beni, S. Czellar, J. Karancsi[21], A. Makovec, J. Molnar, Z. Szillasi

Institute of Physics, University of Debrecen, Debrecen, Hungary
P. Raics, D. Teyssier, Z.L. Trocsanyi, B. Ujvari

Eszterhazy Karoly University, Karoly Robert Campus, Gyongyos, Hungary
T. Csorgo, W.J. Metzger, F. Nemes, T. Novak

Indian Institute of Science (IISc), Bangalore, India
S. Choudhury, J.R. Komaragiri, P.C. Tiwari

National Institute of Science Education and Research, HBNI, Bhubaneswar, India
S. Bahinipati[24], C. Kar, G. Kole, P. Mal, V.K. Muraleedharan Nair Bindhu, A. Nayak[25], D.K. Sahoo[24], S.K. Swain

JHEP03(2020)103

Panjab University, Chandigarh, India
S. Bansal, S.B. Beri, V. Bhatnagar, S. Chauhan, R. Chawla, N. Dhingra, R. Gupta, A. Kaur, M. Kaur, S. Kaur, P. Kumari, M. Lohan, M. Meena, K. Sandeep, S. Sharma, J.B. Singh, A.K. Virdi, G. Walia

University of Delhi, Delhi, India
A. Bhardwaj, B.C. Choudhary, R.B. Garg, M. Gola, S. Keshri, Ashok Kumar, S. Malhotra, M. Naimuddin, P. Priyanka, K. Ranjan, Aashaq Shah, R. Sharma

Saha Institute of Nuclear Physics, HBNI, Kolkata, India
R. Bhardwaj[26], M. Bharti[26], R. Bhattacharya, S. Bhattacharya, U. Bhawandeep[26], D. Bhowmik, S. Dey, S. Dutta, S. Ghosh, M. Maity[27], K. Mondal, S. Nandan, A. Purohit, P.K. Rout, G. Saha, S. Sarkar, T. Sarkar[27], M. Sharan, B. Singh[26], S. Thakur[26]

Indian Institute of Technology Madras, Madras, India
P.K. Behera, P. Kalbhor, A. Muhammad, P.R. Pujahari, A. Sharma, A.K. Sikdar

Bhabha Atomic Research Centre, Mumbai, India
R. Chudasama, D. Dutta, V. Jha, V. Kumar, D.K. Mishra, P.K. Netrakanti, L.M. Pant, P. Shukla

Tata Institute of Fundamental Research-A, Mumbai, India
T. Aziz, M.A. Bhat, S. Dugad, G.B. Mohanty, N. Sur, RavindraKumar Verma

Tata Institute of Fundamental Research-B, Mumbai, India
S. Banerjee, S. Bhattacharya, S. Chatterjee, P. Das, M. Guchait, S. Karmakar, S. Kumar, G. Majumder, K. Mazumdar, N. Sahoo, S. Sawant

Indian Institute of Science Education and Research (IISER), Pune, India
S. Chauhan, S. Dube, V. Hegde, A. Kapoor, K. Kothekar, S. Pandey, A. Rane, A. Rastogi, S. Sharma

Institute for Research in Fundamental Sciences (IPM), Tehran, Iran
S. Chenarani[28], E. Eskandari Tadavani, S.M. Etesami[28], M. Khakzad, M. Mohammadi Najafabadi, M. Naseri, F. Rezaei Hosseinabadi

University College Dublin, Dublin, Ireland
M. Felcini, M. Grunewald

INFN Sezione di Bari [a], Università di Bari [b], Politecnico di Bari [c], Bari, Italy
M. Abbrescia[a,b], R. Aly[a,b,29], C. Calabria[a,b], A. Colaleo[a], D. Creanza[a,c], L. Cristella[a,b], N. De Filippis[a,c], M. De Palma[a,b], A. Di Florio[a,b], L. Fiore[a], A. Gelmi[a,b], G. Iaselli[a,c], M. Ince[a,b], S. Lezki[a,b], G. Maggi[a,c], M. Maggi[a], G. Miniello[a,b], S. My[a,b], S. Nuzzo[a,b], A. Pompili[a,b], G. Pugliese[a,c], R. Radogna[a], A. Ranieri[a], G. Selvaggi[a,b], L. Silvestris[a], R. Venditti[a], P. Verwilligen[a]

INFN Sezione di Bologna [a], Università di Bologna [b], Bologna, Italy
G. Abbiendi[a], C. Battilana[a,b], D. Bonacorsi[a,b], L. Borgonovi[a,b], S. Braibant-Giacomelli[a,b], R. Campanini[a,b], P. Capiluppi[a,b], A. Castro[a,b], F.R. Cavallo[a], C. Ciocca[a], G. Codispoti[a,b],

JHEP03(2020)103

M. Cuffiani[a,b], G.M. Dallavalle[a], F. Fabbri[a], A. Fanfani[a,b], E. Fontanesi, P. Giacomelli[a], C. Grandi[a], L. Guiducci[a,b], F. Iemmi[a,b], S. Lo Meo[a,30], S. Marcellini[a], G. Masetti[a], F.L. Navarria[a,b], A. Perrotta[a], F. Primavera[a,b], A.M. Rossi[a,b], T. Rovelli[a,b], G.P. Siroli[a,b], N. Tosi[a]

INFN Sezione di Catania [a], Università di Catania [b], Catania, Italy
S. Albergo[a,b,31], S. Costa[a,b], A. Di Mattia[a], R. Potenza[a,b], A. Tricomi[a,b,31], C. Tuve[a,b]

INFN Sezione di Firenze [a], Università di Firenze [b], Firenze, Italy
G. Barbagli[a], R. Ceccarelli, K. Chatterjee[a,b], V. Ciulli[a,b], C. Civinini[a], R. D'Alessandro[a,b], E. Focardi[a,b], G. Latino, P. Lenzi[a,b], M. Meschini[a], S. Paoletti[a], G. Sguazzoni[a], D. Strom[a], L. Viliani[a]

INFN Laboratori Nazionali di Frascati, Frascati, Italy
L. Benussi, S. Bianco, D. Piccolo

INFN Sezione di Genova [a], Università di Genova [b], Genova, Italy
M. Bozzo[a,b], F. Ferro[a], R. Mulargia[a,b], E. Robutti[a], S. Tosi[a,b]

INFN Sezione di Milano-Bicocca [a], Università di Milano-Bicocca [b], Milano, Italy
A. Benaglia[a], A. Beschi[a,b], F. Brivio[a,b], V. Ciriolo[a,b,17], S. Di Guida[a,b,17], M.E. Dinardo[a,b], P. Dini[a], S. Fiorendi[a,b], S. Gennai[a], A. Ghezzi[a,b], P. Govoni[a,b], L. Guzzi[a,b], M. Malberti[a], S. Malvezzi[a], D. Menasce[a], F. Monti[a,b], L. Moroni[a], G. Ortona[a,b], M. Paganoni[a,b], D. Pedrini[a], S. Ragazzi[a,b], T. Tabarelli de Fatis[a,b], D. Zuolo[a,b]

INFN Sezione di Napoli [a], Università di Napoli 'Federico II' [b], Napoli, Italy, Università della Basilicata [c], Potenza, Italy, Università G. Marconi [d], Roma, Italy
S. Buontempo[a], N. Cavallo[a,c], A. De Iorio[a,b], A. Di Crescenzo[a,b], F. Fabozzi[a,c], F. Fienga[a], G. Galati[a], A.O.M. Iorio[a,b], L. Lista[a,b], S. Meola[a,d,17], P. Paolucci[a,17], B. Rossi[a], C. Sciacca[a,b], E. Voevodina[a,b]

INFN Sezione di Padova [a], Università di Padova [b], Padova, Italy, Università di Trento [c], Trento, Italy
P. Azzi[a], N. Bacchetta[a], D. Bisello[a,b], A. Boletti[a,b], A. Bragagnolo, R. Carlin[a,b], P. Checchia[a], P. De Castro Manzano[a], T. Dorigo[a], U. Dosselli[a], F. Gasparini[a,b], U. Gasparini[a,b], A. Gozzelino[a], S.Y. Hoh, P. Lujan, M. Margoni[a,b], A.T. Meneguzzo[a,b], J. Pazzini[a,b], M. Presilla[b], P. Ronchese[a,b], R. Rossin[a,b], F. Simonetto[a,b], A. Tiko, M. Tosi[a,b], M. Zanetti[a,b], P. Zotto[a,b], G. Zumerle[a,b]

INFN Sezione di Pavia [a], Università di Pavia [b], Pavia, Italy
A. Braghieri[a], P. Montagna[a,b], S.P. Ratti[a,b], V. Re[a], M. Ressegotti[a,b], C. Riccardi[a,b], P. Salvini[a], I. Vai[a,b], P. Vitulo[a,b]

INFN Sezione di Perugia [a], Università di Perugia [b], Perugia, Italy
M. Biasini[a,b], G.M. Bilei[a], C. Cecchi[a,b], D. Ciangottini[a,b], L. Fanò[a,b], P. Lariccia[a,b], R. Leonardi[a,b], E. Manoni[a], G. Mantovani[a,b], V. Mariani[a,b], M. Menichelli[a], A. Rossi[a,b],

JHEP03(2020)103

A. Santocchia[a,b], D. Spiga[a]

INFN Sezione di Pisa [a], Università di Pisa [b], Scuola Normale Superiore di Pisa [c], Pisa, Italy

K. Androsov[a], P. Azzurri[a], G. Bagliesi[a], V. Bertacchi[a,c], L. Bianchini[a], T. Boccali[a], R. Castaldi[a], M.A. Ciocci[a,b], R. Dell'Orso[a], G. Fedi[a], L. Giannini[a,c], A. Giassi[a], M.T. Grippo[a], F. Ligabue[a,c], E. Manca[a,c], G. Mandorli[a,c], A. Messineo[a,b], F. Palla[a], A. Rizzi[a,b], G. Rolandi[32], S. Roy Chowdhury, A. Scribano[a], P. Spagnolo[a], R. Tenchini[a], G. Tonelli[a,b], N. Turini, A. Venturi[a], P.G. Verdini[a]

INFN Sezione di Roma [a], Sapienza Università di Roma [b], Rome, Italy

F. Cavallari[a], M. Cipriani[a,b], D. Del Re[a,b], E. Di Marco[a,b], M. Diemoz[a], E. Longo[a,b], B. Marzocchi[a,b], P. Meridiani[a], G. Organtini[a,b], F. Pandolfi[a], R. Paramatti[a,b], C. Quaranta[a,b], S. Rahatlou[a,b], C. Rovelli[a], F. Santanastasio[a,b], L. Soffi[a,b]

INFN Sezione di Torino [a], Università di Torino [b], Torino, Italy, Università del Piemonte Orientale [c], Novara, Italy

N. Amapane[a,b], R. Arcidiacono[a,c], S. Argiro[a,b], M. Arneodo[a,c], N. Bartosik[a], R. Bellan[a,b], C. Biino[a], A. Cappati[a,b], N. Cartiglia[a], S. Cometti[a], M. Costa[a,b], R. Covarelli[a,b], N. Demaria[a], B. Kiani[a,b], C. Mariotti[a], S. Maselli[a], E. Migliore[a,b], V. Monaco[a,b], E. Monteil[a,b], M. Monteno[a], M.M. Obertino[a,b], L. Pacher[a,b], N. Pastrone[a], M. Pelliccioni[a], G.L. Pinna Angioni[a,b], A. Romero[a,b], M. Ruspa[a,c], R. Sacchi[a,b], R. Salvatico[a,b], V. Sola[a], A. Solano[a,b], D. Soldi[a,b], A. Staiano[a]

INFN Sezione di Trieste [a], Università di Trieste [b], Trieste, Italy

S. Belforte[a], V. Candelise[a,b], M. Casarsa[a], F. Cossutti[a], A. Da Rold[a,b], G. Della Ricca[a,b], F. Vazzoler[a,b], A. Zanetti[a]

Kyungpook National University, Daegu, Korea

B. Kim, D.H. Kim, G.N. Kim, M.S. Kim, J. Lee, S.W. Lee, C.S. Moon, Y.D. Oh, S.I. Pak, S. Sekmen, D.C. Son, Y.C. Yang

Chonnam National University, Institute for Universe and Elementary Particles, Kwangju, Korea

H. Kim, D.H. Moon, G. Oh

Hanyang University, Seoul, Korea

B. Francois, T.J. Kim, J. Park

Korea University, Seoul, Korea

S. Cho, S. Choi, Y. Go, D. Gyun, S. Ha, B. Hong, K. Lee, K.S. Lee, J. Lim, J. Park, S.K. Park, Y. Roh

Kyung Hee University, Department of Physics

J. Goh

Sejong University, Seoul, Korea

H.S. Kim

JHEP03(2020)103

Seoul National University, Seoul, Korea
J. Almond, J.H. Bhyun, J. Choi, S. Jeon, J. Kim, J.S. Kim, H. Lee, K. Lee, S. Lee, K. Nam, M. Oh, S.B. Oh, B.C. Radburn-Smith, U.K. Yang, H.D. Yoo, I. Yoon, G.B. Yu

University of Seoul, Seoul, Korea
D. Jeon, H. Kim, J.H. Kim, J.S.H. Lee, I.C. Park, I. Watson

Sungkyunkwan University, Suwon, Korea
Y. Choi, C. Hwang, Y. Jeong, J. Lee, Y. Lee, I. Yu

Riga Technical University, Riga, Latvia
V. Veckalns[33]

Vilnius University, Vilnius, Lithuania
V. Dudenas, A. Juodagalvis, G. Tamulaitis, J. Vaitkus

National Centre for Particle Physics, Universiti Malaya, Kuala Lumpur, Malaysia
Z.A. Ibrahim, F. Mohamad Idris[34], W.A.T. Wan Abdullah, M.N. Yusli, Z. Zolkapli

Universidad de Sonora (UNISON), Hermosillo, Mexico
J.F. Benitez, A. Castaneda Hernandez, J.A. Murillo Quijada, L. Valencia Palomo

Centro de Investigacion y de Estudios Avanzados del IPN, Mexico City, Mexico
H. Castilla-Valdez, E. De La Cruz-Burelo, I. Heredia-De La Cruz[35], R. Lopez-Fernandez, A. Sanchez-Hernandez

Universidad Iberoamericana, Mexico City, Mexico
S. Carrillo Moreno, C. Oropeza Barrera, M. Ramirez-Garcia, F. Vazquez Valencia

Benemerita Universidad Autonoma de Puebla, Puebla, Mexico
J. Eysermans, I. Pedraza, H.A. Salazar Ibarguen, C. Uribe Estrada

Universidad Autónoma de San Luis Potosí, San Luis Potosí, Mexico
A. Morelos Pineda

University of Montenegro, Podgorica, Montenegro
N. Raicevic

University of Auckland, Auckland, New Zealand
D. Krofcheck

University of Canterbury, Christchurch, New Zealand
S. Bheesette, P.H. Butler

National Centre for Physics, Quaid-I-Azam University, Islamabad, Pakistan
A. Ahmad, M. Ahmad, Q. Hassan, H.R. Hoorani, W.A. Khan, M.A. Shah, M. Shoaib, M. Waqas

AGH University of Science and Technology Faculty of Computer Science, Electronics and Telecommunications, Krakow, Poland
V. Avati, L. Grzanka, M. Malawski

JHEP03(2020)103

National Centre for Nuclear Research, Swierk, Poland

H. Bialkowska, M. Bluj, B. Boimska, M. Górski, M. Kazana, M. Szleper, P. Zalewski

Institute of Experimental Physics, Faculty of Physics, University of Warsaw, Warsaw, Poland

K. Bunkowski, A. Byszuk[36], K. Doroba, A. Kalinowski, M. Konecki, J. Krolikowski, M. Misiura, M. Olszewski, A. Pyskir, M. Walczak

Laboratório de Instrumentação e Física Experimental de Partículas, Lisboa, Portugal

M. Araujo, P. Bargassa, D. Bastos, A. Di Francesco, P. Faccioli, B. Galinhas, M. Gallinaro, J. Hollar, N. Leonardo, J. Seixas, K. Shchelina, G. Strong, O. Toldaiev, J. Varela

Joint Institute for Nuclear Research, Dubna, Russia

A. Baginyan, Y. Ershov, M. Gavrilenko, A. Golunov, I. Golutvin, N. Gorbounov, I. Gorbunov, V. Karjavine, A. Lanev, A. Malakhov, V. Matveev[37,38], V.V. Mitsyn, P. Moisenz, V. Palichik, V. Perelygin, M. Savina, S. Shmatov, S. Shulha, N. Voytishin, A. Zarubin

Petersburg Nuclear Physics Institute, Gatchina (St. Petersburg), Russia

L. Chtchipounov, V. Golovtsov, Y. Ivanov, V. Kim[39], E. Kuznetsova[40], P. Levchenko, V. Murzin, V. Oreshkin, I. Smirnov, D. Sosnov, V. Sulimov, L. Uvarov, A. Vorobyev

Institute for Nuclear Research, Moscow, Russia

Yu. Andreev, A. Dermenev, S. Gninenko, N. Golubev, A. Karneyeu, M. Kirsanov, N. Krasnikov, A. Pashenkov, D. Tlisov, A. Toropin

Institute for Theoretical and Experimental Physics named by A.I. Alikhanov of NRC 'Kurchatov Institute', Moscow, Russia

V. Epshteyn, V. Gavrilov, N. Lychkovskaya, A. Nikitenko[41], V. Popov, I. Pozdnyakov, G. Safronov, A. Spiridonov, A. Stepennov, M. Toms, E. Vlasov, A. Zhokin

Moscow Institute of Physics and Technology, Moscow, Russia

T. Aushev

National Research Nuclear University 'Moscow Engineering Physics Institute' (MEPhI), Moscow, Russia

M. Chadeeva[42], P. Parygin, D. Philippov, E. Popova, V. Rusinov

P.N. Lebedev Physical Institute, Moscow, Russia

V. Andreev, M. Azarkin, I. Dremin, M. Kirakosyan, A. Terkulov

Skobeltsyn Institute of Nuclear Physics, Lomonosov Moscow State University, Moscow, Russia

A. Baskakov, A. Belyaev, E. Boos, V. Bunichev, M. Dubinin[43], L. Dudko, V. Klyukhin, O. Kodolova, I. Lokhtin, S. Obraztsov, M. Perfilov, S. Petrushanko, V. Savrin

Novosibirsk State University (NSU), Novosibirsk, Russia

A. Barnyakov[44], V. Blinov[44], T. Dimova[44], L. Kardapoltsev[44], Y. Skovpen[44]

JHEP03(2020)103

Institute for High Energy Physics of National Research Centre 'Kurchatov Institute', Protvino, Russia

I. Azhgirey, I. Bayshev, S. Bitioukov, V. Kachanov, D. Konstantinov, P. Mandrik, V. Petrov, R. Ryutin, S. Slabospitskii, A. Sobol, S. Troshin, N. Tyurin, A. Uzunian, A. Volkov

National Research Tomsk Polytechnic University, Tomsk, Russia

A. Babaev, A. Iuzhakov, V. Okhotnikov

Tomsk State University, Tomsk, Russia

V. Borchsh, V. Ivanchenko, E. Tcherniaev

University of Belgrade: Faculty of Physics and VINCA Institute of Nuclear Sciences

P. Adzic[45], P. Cirkovic, D. Devetak, M. Dordevic, P. Milenovic, J. Milosevic, M. Stojanovic

Centro de Investigaciones Energéticas Medioambientales y Tecnológicas (CIEMAT), Madrid, Spain

M. Aguilar-Benitez, J. Alcaraz Maestre, A. Álvarez Fernández, I. Bachiller, M. Barrio Luna, J.A. Brochero Cifuentes, C.A. Carrillo Montoya, M. Cepeda, M. Cerrada, N. Colino, B. De La Cruz, A. Delgado Peris, C. Fernandez Bedoya, J.P. Fernández Ramos, J. Flix, M.C. Fouz, O. Gonzalez Lopez, S. Goy Lopez, J.M. Hernandez, M.I. Josa, D. Moran, Á. Navarro Tobar, A. Pérez-Calero Yzquierdo, J. Puerta Pelayo, I. Redondo, L. Romero, S. Sánchez Navas, M.S. Soares, A. Triossi, C. Willmott

Universidad Autónoma de Madrid, Madrid, Spain

C. Albajar, J.F. de Trocóniz

Universidad de Oviedo, Instituto Universitario de Ciencias y Tecnologías Espaciales de Asturias (ICTEA), Oviedo, Spain

B. Alvarez Gonzalez, J. Cuevas, C. Erice, J. Fernandez Menendez, S. Folgueras, I. Gonzalez Caballero, J.R. González Fernández, E. Palencia Cortezon, V. Rodríguez Bouza, S. Sanchez Cruz

Instituto de Física de Cantabria (IFCA), CSIC-Universidad de Cantabria, Santander, Spain

I.J. Cabrillo, A. Calderon, B. Chazin Quero, J. Duarte Campderros, M. Fernandez, P.J. Fernández Manteca, A. García Alonso, G. Gomez, C. Martinez Rivero, P. Martinez Ruiz del Arbol, F. Matorras, J. Piedra Gomez, C. Prieels, T. Rodrigo, A. Ruiz-Jimeno, L. Russo[46], L. Scodellaro, N. Trevisani, I. Vila, J.M. Vizan Garcia

University of Colombo, Colombo, Sri Lanka

K. Malagalage

University of Ruhuna, Department of Physics, Matara, Sri Lanka

W.G.D. Dharmaratna, N. Wickramage

JHEP03(2020)103

CERN, European Organization for Nuclear Research, Geneva, Switzerland

D. Abbaneo, B. Akgun, E. Auffray, G. Auzinger, J. Baechler, P. Baillon, A.H. Ball, D. Barney, J. Bendavid, M. Bianco, A. Bocci, P. Bortignon, E. Bossini, C. Botta, E. Brondolin, T. Camporesi, A. Caratelli, G. Cerminara, E. Chapon, G. Cucciati, D. d'Enterria, A. Dabrowski, N. Daci, V. Daponte, A. David, O. Davignon, A. De Roeck, N. Deelen, M. Deile, M. Dobson, M. Dünser, N. Dupont, A. Elliott-Peisert, F. Fallavollita[47], D. Fasanella, G. Franzoni, J. Fulcher, W. Funk, S. Giani, D. Gigi, A. Gilbert, K. Gill, F. Glege, M. Gruchala, M. Guilbaud, D. Gulhan, J. Hegeman, C. Heidegger, Y. Iiyama, V. Innocente, P. Janot, O. Karacheban[20], J. Kaspar, J. Kieseler, M. Krammer[1], C. Lange, P. Lecoq, C. Lourenço, L. Malgeri, M. Mannelli, A. Massironi, F. Meijers, J.A. Merlin, S. Mersi, E. Meschi, F. Moortgat, M. Mulders, J. Ngadiuba, S. Nourbakhsh, S. Orfanelli, L. Orsini, F. Pantaleo[17], L. Pape, E. Perez, M. Peruzzi, A. Petrilli, G. Petrucciani, A. Pfeiffer, M. Pierini, F.M. Pitters, D. Rabady, A. Racz, M. Rovere, H. Sakulin, C. Schäfer, C. Schwick, M. Selvaggi, A. Sharma, P. Silva, W. Snoeys, P. Sphicas[48], J. Steggemann, V.R. Tavolaro, D. Treille, A. Tsirou, A. Vartak, M. Verzetti, W.D. Zeuner

Paul Scherrer Institut, Villigen, Switzerland

L. Caminada[49], K. Deiters, W. Erdmann, R. Horisberger, Q. Ingram, H.C. Kaestli, D. Kotlinski, U. Langenegger, T. Rohe, S.A. Wiederkehr

ETH Zurich — Institute for Particle Physics and Astrophysics (IPA), Zurich, Switzerland

M. Backhaus, P. Berger, N. Chernyavskaya, G. Dissertori, M. Dittmar, M. Donegà, C. Dorfer, T.A. Gómez Espinosa, C. Grab, D. Hits, T. Klijnsma, W. Lustermann, R.A. Manzoni, M. Marionneau, M.T. Meinhard, F. Micheli, P. Musella, F. Nessi-Tedaldi, F. Pauss, G. Perrin, L. Perrozzi, S. Pigazzini, M. Reichmann, C. Reissel, T. Reitenspiess, D. Ruini, D.A. Sanz Becerra, M. Schönenberger, L. Shchutska, M.L. Vesterbacka Olsson, R. Wallny, D.H. Zhu

Universität Zürich, Zurich, Switzerland

T.K. Aarrestad, C. Amsler[50], D. Brzhechko, M.F. Canelli, A. De Cosa, R. Del Burgo, S. Donato, B. Kilminster, S. Leontsinis, V.M. Mikuni, I. Neutelings, G. Rauco, P. Robmann, D. Salerno, K. Schweiger, C. Seitz, Y. Takahashi, S. Wertz, A. Zucchetta

National Central University, Chung-Li, Taiwan

T.H. Doan, C.M. Kuo, W. Lin, A. Roy, S.S. Yu

National Taiwan University (NTU), Taipei, Taiwan

P. Chang, Y. Chao, K.F. Chen, P.H. Chen, W.-S. Hou, Y.y. Li, R.-S. Lu, E. Paganis, A. Psallidas, A. Steen

Chulalongkorn University, Faculty of Science, Department of Physics, Bangkok, Thailand

B. Asavapibhop, C. Asawatangtrakuldee, N. Srimanobhas, N. Suwonjandee

JHEP03(2020)103

Çukurova University, Physics Department, Science and Art Faculty, Adana, Turkey

A. Bat, F. Boran, S. Cerci[51], S. Damarseckin[52], Z.S. Demiroglu, F. Dolek, C. Dozen, I. Dumanoglu, G. Gokbulut, EmineGurpinar Guler[53], Y. Guler, I. Hos[54], C. Isik, E.E. Kangal[55], O. Kara, A. Kayis Topaksu, U. Kiminsu, M. Oglakci, G. Onengut, K. Ozdemir[56], S. Ozturk[57], A.E. Simsek, D. Sunar Cerci[51], U.G. Tok, S. Turkcapar, I.S. Zorbakir, C. Zorbilmez

Middle East Technical University, Physics Department, Ankara, Turkey

B. Isildak[58], G. Karapinar[59], M. Yalvac

Bogazici University, Istanbul, Turkey

I.O. Atakisi, E. Gülmez, M. Kaya[60], O. Kaya[61], B. Kaynak, Ö. Özçelik, S. Tekten, E.A. Yetkin[62]

Istanbul Technical University, Istanbul, Turkey

A. Cakir, K. Cankocak, Y. Komurcu, S. Sen[63]

Istanbul University, Istanbul, Turkey

S. Ozkorucuklu

Institute for Scintillation Materials of National Academy of Science of Ukraine, Kharkov, Ukraine

B. Grynyov

National Scientific Center, Kharkov Institute of Physics and Technology, Kharkov, Ukraine

L. Levchuk

University of Bristol, Bristol, United Kingdom

F. Ball, E. Bhal, S. Bologna, J.J. Brooke, D. Burns, E. Clement, D. Cussans, H. Flacher, J. Goldstein, G.P. Heath, H.F. Heath, L. Kreczko, S. Paramesvaran, B. Penning, T. Sakuma, S. Seif El Nasr-Storey, D. Smith, V.J. Smith, J. Taylor, A. Titterton

Rutherford Appleton Laboratory, Didcot, United Kingdom

K.W. Bell, A. Belyaev[64], C. Brew, R.M. Brown, D. Cieri, D.J.A. Cockerill, J.A. Coughlan, K. Harder, S. Harper, J. Linacre, K. Manolopoulos, D.M. Newbold, E. Olaiya, D. Petyt, T. Reis, T. Schuh, C.H. Shepherd-Themistocleous, A. Thea, I.R. Tomalin, T. Williams, W.J. Womersley

Imperial College, London, United Kingdom

R. Bainbridge, P. Bloch, J. Borg, S. Breeze, O. Buchmuller, A. Bundock, GurpreetSingh CHAHAL[65], D. Colling, P. Dauncey, G. Davies, M. Della Negra, R. Di Maria, P. Everaerts, G. Hall, G. Iles, T. James, M. Komm, C. Laner, L. Lyons, A.-M. Magnan, S. Malik, A. Martelli, V. Milosevic, J. Nash[66], V. Palladino, M. Pesaresi, D.M. Raymond, A. Richards, A. Rose, E. Scott, C. Seez, A. Shtipliyski, M. Stoye, T. Strebler, S. Summers, A. Tapper, K. Uchida, T. Virdee[17], N. Wardle, D. Winterbottom, J. Wright, A.G. Zecchinelli, S.C. Zenz

JHEP03(2020)103

Brunel University, Uxbridge, United Kingdom

J.E. Cole, P.R. Hobson, A. Khan, P. Kyberd, C.K. Mackay, A. Morton, I.D. Reid, L. Teodorescu, S. Zahid

Baylor University, Waco, U.S.A.

K. Call, J. Dittmann, K. Hatakeyama, C. Madrid, B. McMaster, N. Pastika, C. Smith

Catholic University of America, Washington, DC, U.S.A.

R. Bartek, A. Dominguez, R. Uniyal

The University of Alabama, Tuscaloosa, U.S.A.

A. Buccilli, S.I. Cooper, C. Henderson, P. Rumerio, C. West

Boston University, Boston, U.S.A.

D. Arcaro, T. Bose, Z. Demiragli, D. Gastler, S. Girgis, D. Pinna, C. Richardson, J. Rohlf, D. Sperka, I. Suarez, L. Sulak, D. Zou

Brown University, Providence, U.S.A.

G. Benelli, B. Burkle, X. Coubez, D. Cutts, Y.t. Duh, M. Hadley, J. Hakala, U. Heintz, J.M. Hogan[67], K.H.M. Kwok, E. Laird, G. Landsberg, J. Lee, Z. Mao, M. Narain, S. Sagir[68], R. Syarif, E. Usai, D. Yu

University of California, Davis, Davis, U.S.A.

R. Band, C. Brainerd, R. Breedon, M. Calderon De La Barca Sanchez, M. Chertok, J. Conway, R. Conway, P.T. Cox, R. Erbacher, C. Flores, G. Funk, F. Jensen, W. Ko, O. Kukral, R. Lander, M. Mulhearn, D. Pellett, J. Pilot, M. Shi, D. Stolp, D. Taylor, K. Tos, M. Tripathi, Z. Wang, F. Zhang

University of California, Los Angeles, U.S.A.

M. Bachtis, C. Bravo, R. Cousins, A. Dasgupta, A. Florent, J. Hauser, M. Ignatenko, N. Mccoll, W.A. Nash, S. Regnard, D. Saltzberg, C. Schnaible, B. Stone, V. Valuev

University of California, Riverside, Riverside, U.S.A.

K. Burt, R. Clare, J.W. Gary, S.M.A. Ghiasi Shirazi, G. Hanson, G. Karapostoli, E. Kennedy, O.R. Long, M. Olmedo Negrete, M.I. Paneva, W. Si, L. Wang, H. Wei, S. Wimpenny, B.R. Yates, Y. Zhang

University of California, San Diego, La Jolla, U.S.A.

J.G. Branson, P. Chang, S. Cittolin, M. Derdzinski, R. Gerosa, D. Gilbert, B. Hashemi, D. Klein, V. Krutelyov, J. Letts, M. Masciovecchio, S. May, S. Padhi, M. Pieri, V. Sharma, M. Tadel, F. Würthwein, A. Yagil, G. Zevi Della Porta

University of California, Santa Barbara — Department of Physics, Santa Barbara, U.S.A.

N. Amin, R. Bhandari, C. Campagnari, M. Citron, V. Dutta, M. Franco Sevilla, L. Gouskos, J. Incandela, B. Marsh, H. Mei, A. Ovcharova, H. Qu, J. Richman, U. Sarica, D. Stuart, S. Wang, J. Yoo

JHEP03(2020)103

California Institute of Technology, Pasadena, U.S.A.

D. Anderson, A. Bornheim, O. Cerri, I. Dutta, J.M. Lawhorn, N. Lu, J. Mao, H.B. Newman, T.Q. Nguyen, J. Pata, M. Spiropulu, J.R. Vlimant, S. Xie, Z. Zhang, R.Y. Zhu

Carnegie Mellon University, Pittsburgh, U.S.A.

M.B. Andrews, T. Ferguson, T. Mudholkar, M. Paulini, M. Sun, I. Vorobiev, M. Weinberg

University of Colorado Boulder, Boulder, U.S.A.

J.P. Cumalat, W.T. Ford, A. Johnson, E. MacDonald, T. Mulholland, R. Patel, A. Perloff, K. Stenson, K.A. Ulmer, S.R. Wagner

Cornell University, Ithaca, U.S.A.

J. Alexander, J. Chaves, Y. Cheng, J. Chu, A. Datta, A. Frankenthal, K. Mcdermott, N. Mirman, J.R. Patterson, D. Quach, A. Rinkevicius[69], A. Ryd, S.M. Tan, Z. Tao, J. Thom, P. Wittich, M. Zientek

Fermi National Accelerator Laboratory, Batavia, U.S.A.

S. Abdullin, M. Albrow, M. Alyari, G. Apollinari, A. Apresyan, A. Apyan, S. Banerjee, L.A.T. Bauerdick, A. Beretvas, J. Berryhill, P.C. Bhat, K. Burkett, J.N. Butler, A. Canepa, G.B. Cerati, H.W.K. Cheung, F. Chlebana, M. Cremonesi, J. Duarte, V.D. Elvira, J. Freeman, Z. Gecse, E. Gottschalk, L. Gray, D. Green, S. Grünendahl, O. Gutsche, AllisonReinsvold Hall, J. Hanlon, R.M. Harris, S. Hasegawa, R. Heller, J. Hirschauer, B. Jayatilaka, S. Jindariani, M. Johnson, U. Joshi, B. Klima, M.J. Kortelainen, B. Kreis, S. Lammel, J. Lewis, D. Lincoln, R. Lipton, M. Liu, T. Liu, J. Lykken, K. Maeshima, J.M. Marraffino, D. Mason, P. McBride, P. Merkel, S. Mrenna, S. Nahn, V. O'Dell, V. Papadimitriou, K. Pedro, C. Pena, G. Rakness, F. Ravera, L. Ristori, B. Schneider, E. Sexton-Kennedy, N. Smith, A. Soha, W.J. Spalding, L. Spiegel, S. Stoynev, J. Strait, N. Strobbe, L. Taylor, S. Tkaczyk, N.V. Tran, L. Uplegger, E.W. Vaandering, C. Vernieri, M. Verzocchi, R. Vidal, M. Wang, H.A. Weber

University of Florida, Gainesville, U.S.A.

D. Acosta, P. Avery, D. Bourilkov, A. Brinkerhoff, L. Cadamuro, A. Carnes, V. Cherepanov, D. Curry, F. Errico, R.D. Field, S.V. Gleyzer, B.M. Joshi, M. Kim, J. Konigsberg, A. Korytov, K.H. Lo, P. Ma, K. Matchev, N. Menendez, G. Mitselmakher, D. Rosenzweig, K. Shi, J. Wang, S. Wang, X. Zuo

Florida International University, Miami, U.S.A.

Y.R. Joshi

Florida State University, Tallahassee, U.S.A.

T. Adams, A. Askew, S. Hagopian, V. Hagopian, K.F. Johnson, R. Khurana, T. Kolberg, G. Martinez, T. Perry, H. Prosper, C. Schiber, R. Yohay, J. Zhang

Florida Institute of Technology, Melbourne, U.S.A.

M.M. Baarmand, V. Bhopatkar, M. Hohlmann, D. Noonan, M. Rahmani, M. Saunders, F. Yumiceva

JHEP03(2020)103

University of Illinois at Chicago (UIC), Chicago, U.S.A.
M.R. Adams, L. Apanasevich, D. Berry, R.R. Betts, R. Cavanaugh, X. Chen, S. Dittmer, O. Evdokimov, C.E. Gerber, D.A. Hangal, D.J. Hofman, K. Jung, C. Mills, T. Roy, M.B. Tonjes, N. Varelas, H. Wang, X. Wang, Z. Wu

The University of Iowa, Iowa City, U.S.A.
M. Alhusseini, B. Bilki[53], W. Clarida, K. Dilsiz[70], S. Durgut, R.P. Gandrajula, M. Haytmyradov, V. Khristenko, O.K. Köseyan, J.-P. Merlo, A. Mestvirishvili[71], A. Moeller, J. Nachtman, H. Ogul[72], Y. Onel, F. Ozok[73], A. Penzo, C. Snyder, E. Tiras, J. Wetzel

Johns Hopkins University, Baltimore, U.S.A.
B. Blumenfeld, A. Cocoros, N. Eminizer, D. Fehling, L. Feng, A.V. Gritsan, W.T. Hung, P. Maksimovic, J. Roskes, M. Swartz, M. Xiao

The University of Kansas, Lawrence, U.S.A.
C. Baldenegro Barrera, P. Baringer, A. Bean, S. Boren, J. Bowen, A. Bylinkin, T. Isidori, S. Khalil, J. King, G. Krintiras, A. Kropivnitskaya, C. Lindsey, D. Majumder, W. Mcbrayer, N. Minafra, M. Murray, C. Rogan, C. Royon, S. Sanders, E. Schmitz, J.D. Tapia Takaki, Q. Wang, J. Williams, G. Wilson

Kansas State University, Manhattan, U.S.A.
S. Duric, A. Ivanov, K. Kaadze, D. Kim, Y. Maravin, D.R. Mendis, T. Mitchell, A. Modak, A. Mohammadi

Lawrence Livermore National Laboratory, Livermore, U.S.A.
F. Rebassoo, D. Wright

University of Maryland, College Park, U.S.A.
A. Baden, O. Baron, A. Belloni, S.C. Eno, Y. Feng, N.J. Hadley, S. Jabeen, G.Y. Jeng, R.G. Kellogg, J. Kunkle, A.C. Mignerey, S. Nabili, F. Ricci-Tam, M. Seidel, Y.H. Shin, A. Skuja, S.C. Tonwar, K. Wong

Massachusetts Institute of Technology, Cambridge, U.S.A.
D. Abercrombie, B. Allen, A. Baty, R. Bi, S. Brandt, W. Busza, I.A. Cali, M. D'Alfonso, G. Gomez Ceballos, M. Goncharov, P. Harris, D. Hsu, M. Hu, M. Klute, D. Kovalskyi, Y.-J. Lee, P.D. Luckey, B. Maier, A.C. Marini, C. Mcginn, C. Mironov, S. Narayanan, X. Niu, C. Paus, D. Rankin, C. Roland, G. Roland, Z. Shi, G.S.F. Stephans, K. Sumorok, K. Tatar, D. Velicanu, J. Wang, T.W. Wang, B. Wyslouch

University of Minnesota, Minneapolis, U.S.A.
A.C. Benvenuti[†], R.M. Chatterjee, A. Evans, S. Guts, P. Hansen, J. Hiltbrand, Sh. Jain, S. Kalafut, Y. Kubota, Z. Lesko, J. Mans, R. Rusack, M.A. Wadud

University of Mississippi, Oxford, U.S.A.
J.G. Acosta, S. Oliveros

University of Nebraska-Lincoln, Lincoln, U.S.A.
K. Bloom, D.R. Claes, C. Fangmeier, L. Finco, F. Golf, R. Gonzalez Suarez, R. Kamalieddin, I. Kravchenko, J.E. Siado, G.R. Snow, B. Stieger

JHEP03(2020)103

State University of New York at Buffalo, Buffalo, U.S.A.

G. Agarwal, C. Harrington, I. Iashvili, A. Kharchilava, C. Mclean, D. Nguyen, A. Parker, J. Pekkanen, S. Rappoccio, B. Roozbahani

Northeastern University, Boston, U.S.A.

G. Alverson, E. Barberis, C. Freer, Y. Haddad, A. Hortiangtham, G. Madigan, D.M. Morse, T. Orimoto, L. Skinnari, A. Tishelman-Charny, T. Wamorkar, B. Wang, A. Wisecarver, D. Wood

Northwestern University, Evanston, U.S.A.

S. Bhattacharya, J. Bueghly, T. Gunter, K.A. Hahn, N. Odell, M.H. Schmitt, K. Sung, M. Trovato, M. Velasco

University of Notre Dame, Notre Dame, U.S.A.

R. Bucci, N. Dev, R. Goldouzian, M. Hildreth, K. Hurtado Anampa, C. Jessop, D.J. Karmgard, K. Lannon, W. Li, N. Loukas, N. Marinelli, I. Mcalister, F. Meng, C. Mueller, Y. Musienko[37], M. Planer, R. Ruchti, P. Siddireddy, G. Smith, S. Taroni, M. Wayne, A. Wightman, M. Wolf, A. Woodard

The Ohio State University, Columbus, U.S.A.

J. Alimena, B. Bylsma, L.S. Durkin, S. Flowers, B. Francis, C. Hill, W. Ji, A. Lefeld, T.Y. Ling, B.L. Winer

Princeton University, Princeton, U.S.A.

S. Cooperstein, G. Dezoort, P. Elmer, J. Hardenbrook, N. Haubrich, S. Higginbotham, A. Kalogeropoulos, S. Kwan, D. Lange, M.T. Lucchini, J. Luo, D. Marlow, K. Mei, I. Ojalvo, J. Olsen, C. Palmer, P. Piroué, J. Salfeld-Nebgen, D. Stickland, C. Tully, Z. Wang

University of Puerto Rico, Mayaguez, U.S.A.

S. Malik, S. Norberg

Purdue University, West Lafayette, U.S.A.

A. Barker, V.E. Barnes, S. Das, L. Gutay, M. Jones, A.W. Jung, A. Khatiwada, B. Mahakud, D.H. Miller, G. Negro, N. Neumeister, C.C. Peng, S. Piperov, H. Qiu, J.F. Schulte, J. Sun, F. Wang, R. Xiao, W. Xie

Purdue University Northwest, Hammond, U.S.A.

T. Cheng, J. Dolen, N. Parashar

Rice University, Houston, U.S.A.

K.M. Ecklund, S. Freed, F.J.M. Geurts, M. Kilpatrick, Arun Kumar, W. Li, B.P. Padley, R. Redjimi, J. Roberts, J. Rorie, W. Shi, A.G. Stahl Leiton, Z. Tu, A. Zhang

University of Rochester, Rochester, U.S.A.

A. Bodek, P. de Barbaro, R. Demina, J.L. Dulemba, C. Fallon, T. Ferbel, M. Galanti, A. Garcia-Bellido, J. Han, O. Hindrichs, A. Khukhunaishvili, E. Ranken, P. Tan, R. Taus

JHEP03(2020)103

Rutgers, The State University of New Jersey, Piscataway, U.S.A.
B. Chiarito, J.P. Chou, A. Gandrakota, Y. Gershtein, E. Halkiadakis, A. Hart, M. Heindl, E. Hughes, S. Kaplan, S. Kyriacou, I. Laflotte, A. Lath, R. Montalvo, K. Nash, M. Osherson, H. Saka, S. Salur, S. Schnetzer, D. Sheffield, S. Somalwar, R. Stone, S. Thomas, P. Thomassen

University of Tennessee, Knoxville, U.S.A.
H. Acharya, A.G. Delannoy, J. Heideman, G. Riley, S. Spanier

Texas A&M University, College Station, U.S.A.
O. Bouhali[74], A. Celik, M. Dalchenko, M. De Mattia, A. Delgado, S. Dildick, R. Eusebi, J. Gilmore, T. Huang, T. Kamon[75], S. Luo, D. Marley, R. Mueller, D. Overton, L. Perniè, D. Rathjens, A. Safonov

Texas Tech University, Lubbock, U.S.A.
N. Akchurin, J. Damgov, F. De Guio, S. Kunori, K. Lamichhane, S.W. Lee, T. Mengke, S. Muthumuni, T. Peltola, S. Undleeb, I. Volobouev, Z. Wang, A. Whitbeck

Vanderbilt University, Nashville, U.S.A.
S. Greene, A. Gurrola, R. Janjam, W. Johns, C. Maguire, A. Melo, H. Ni, K. Padeken, F. Romeo, P. Sheldon, S. Tuo, J. Velkovska, M. Verweij

University of Virginia, Charlottesville, U.S.A.
M.W. Arenton, P. Barria, B. Cox, G. Cummings, R. Hirosky, M. Joyce, A. Ledovskoy, C. Neu, B. Tannenwald, Y. Wang, E. Wolfe, F. Xia

Wayne State University, Detroit, U.S.A.
R. Harr, P.E. Karchin, N. Poudyal, J. Sturdy, P. Thapa, S. Zaleski

University of Wisconsin — Madison, Madison, WI, U.S.A.
J. Buchanan, C. Caillol, D. Carlsmith, S. Dasu, I. De Bruyn, L. Dodd, F. Fiori, C. Galloni, B. Gomber[76], H. He, M. Herndon, A. Hervé, U. Hussain, P. Klabbers, A. Lanaro, A. Loeliger, K. Long, R. Loveless, J. Madhusudanan Sreekala, T. Ruggles, A. Savin, V. Sharma, W.H. Smith, D. Teague, S. Trembath-reichert, N. Woods

†: Deceased
1: Also at Vienna University of Technology, Vienna, Austria
2: Also at IRFU, CEA, Université Paris-Saclay, Gif-sur-Yvette, France
3: Also at Universidade Estadual de Campinas, Campinas, Brazil
4: Also at Federal University of Rio Grande do Sul, Porto Alegre, Brazil
5: Also at UFMS, Nova Andradina, Brazil
6: Also at Universidade Federal de Pelotas, Pelotas, Brazil
7: Also at Université Libre de Bruxelles, Bruxelles, Belgium
8: Also at University of Chinese Academy of Sciences, Beijing, China
9: Also at Institute for Theoretical and Experimental Physics named by A.I. Alikhanov of NRC 'Kurchatov Institute', Moscow, Russia
10: Also at Joint Institute for Nuclear Research, Dubna, Russia
11: Also at Cairo University, Cairo, Egypt

JHEP03(2020)103

12: Also at British University in Egypt, Cairo, Egypt
13: Now at Ain Shams University, Cairo, Egypt
14: Also at Purdue University, West Lafayette, U.S.A.
15: Also at Université de Haute Alsace, Mulhouse, France
16: Also at Erzincan Binali Yildirim University, Erzincan, Turkey
17: Also at CERN, European Organization for Nuclear Research, Geneva, Switzerland
18: Also at RWTH Aachen University, III. Physikalisches Institut A, Aachen, Germany
19: Also at University of Hamburg, Hamburg, Germany
20: Also at Brandenburg University of Technology, Cottbus, Germany
21: Also at Institute of Physics, University of Debrecen, Debrecen, Hungary, Debrecen, Hungary
22: Also at Institute of Nuclear Research ATOMKI, Debrecen, Hungary
23: Also at MTA-ELTE Lendület CMS Particle and Nuclear Physics Group, Eötvös Loránd University, Budapest, Hungary, Budapest, Hungary
24: Also at IIT Bhubaneswar, Bhubaneswar, India, Bhubaneswar, India
25: Also at Institute of Physics, Bhubaneswar, India
26: Also at Shoolini University, Solan, India
27: Also at University of Visva-Bharati, Santiniketan, India
28: Also at Isfahan University of Technology, Isfahan, Iran
29: Now at INFN Sezione di Bari [a], Università di Bari [b], Politecnico di Bari [c], Bari, Italy
30: Also at Italian National Agency for New Technologies, Energy and Sustainable Economic Development, Bologna, Italy
31: Also at Centro Siciliano di Fisica Nucleare e di Struttura Della Materia, Catania, Italy
32: Also at Scuola Normale e Sezione dell'INFN, Pisa, Italy
33: Also at Riga Technical University, Riga, Latvia, Riga, Latvia
34: Also at Malaysian Nuclear Agency, MOSTI, Kajang, Malaysia
35: Also at Consejo Nacional de Ciencia y Tecnología, Mexico City, Mexico
36: Also at Warsaw University of Technology, Institute of Electronic Systems, Warsaw, Poland
37: Also at Institute for Nuclear Research, Moscow, Russia
38: Now at National Research Nuclear University 'Moscow Engineering Physics Institute' (MEPhI), Moscow, Russia
39: Also at St. Petersburg State Polytechnical University, St. Petersburg, Russia
40: Also at University of Florida, Gainesville, U.S.A.
41: Also at Imperial College, London, United Kingdom
42: Also at P.N. Lebedev Physical Institute, Moscow, Russia
43: Also at California Institute of Technology, Pasadena, U.S.A.
44: Also at Budker Institute of Nuclear Physics, Novosibirsk, Russia
45: Also at Faculty of Physics, University of Belgrade, Belgrade, Serbia
46: Also at Università degli Studi di Siena, Siena, Italy
47: Also at INFN Sezione di Pavia [a], Università di Pavia [b], Pavia, Italy, Pavia, Italy
48: Also at National and Kapodistrian University of Athens, Athens, Greece
49: Also at Universität Zürich, Zurich, Switzerland
50: Also at Stefan Meyer Institute for Subatomic Physics, Vienna, Austria, Vienna, Austria
51: Also at Adiyaman University, Adiyaman, Turkey
52: Also at Şırnak University, Sirnak, Turkey
53: Also at Beykent University, Istanbul, Turkey, Istanbul, Turkey
54: Also at Istanbul Aydin University, Application and Research Center for Advanced Studies (Appendix & Res. Cent. for Advanced Studies), Istanbul, Turkey
55: Also at Mersin University, Mersin, Turkey

JHEP03(2020)103

56: Also at Piri Reis University, Istanbul, Turkey
57: Also at Gaziosmanpasa University, Tokat, Turkey
58: Also at Ozyegin University, Istanbul, Turkey
59: Also at Izmir Institute of Technology, Izmir, Turkey
60: Also at Marmara University, Istanbul, Turkey
61: Also at Kafkas University, Kars, Turkey
62: Also at Istanbul Bilgi University, Istanbul, Turkey
63: Also at Hacettepe University, Ankara, Turkey
64: Also at School of Physics and Astronomy, University of Southampton, Southampton, United Kingdom
65: Also at IPPP Durham University, Durham, United Kingdom
66: Also at Monash University, Faculty of Science, Clayton, Australia
67: Also at Bethel University, St. Paul, Minneapolis, U.S.A., St. Paul, U.S.A.
68: Also at Karamanoğlu Mehmetbey University, Karaman, Turkey
69: Also at Vilnius University, Vilnius, Lithuania
70: Also at Bingol University, Bingol, Turkey
71: Also at Georgian Technical University, Tbilisi, Georgia
72: Also at Sinop University, Sinop, Turkey
73: Also at Mimar Sinan University, Istanbul, Istanbul, Turkey
74: Also at Texas A&M University at Qatar, Doha, Qatar
75: Also at Kyungpook National University, Daegu, Korea, Daegu, Korea
76: Also at University of Hyderabad, Hyderabad, India

JHEP03(2020)103